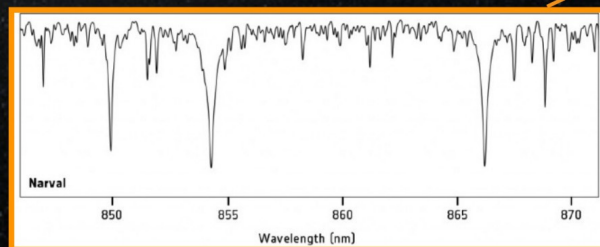
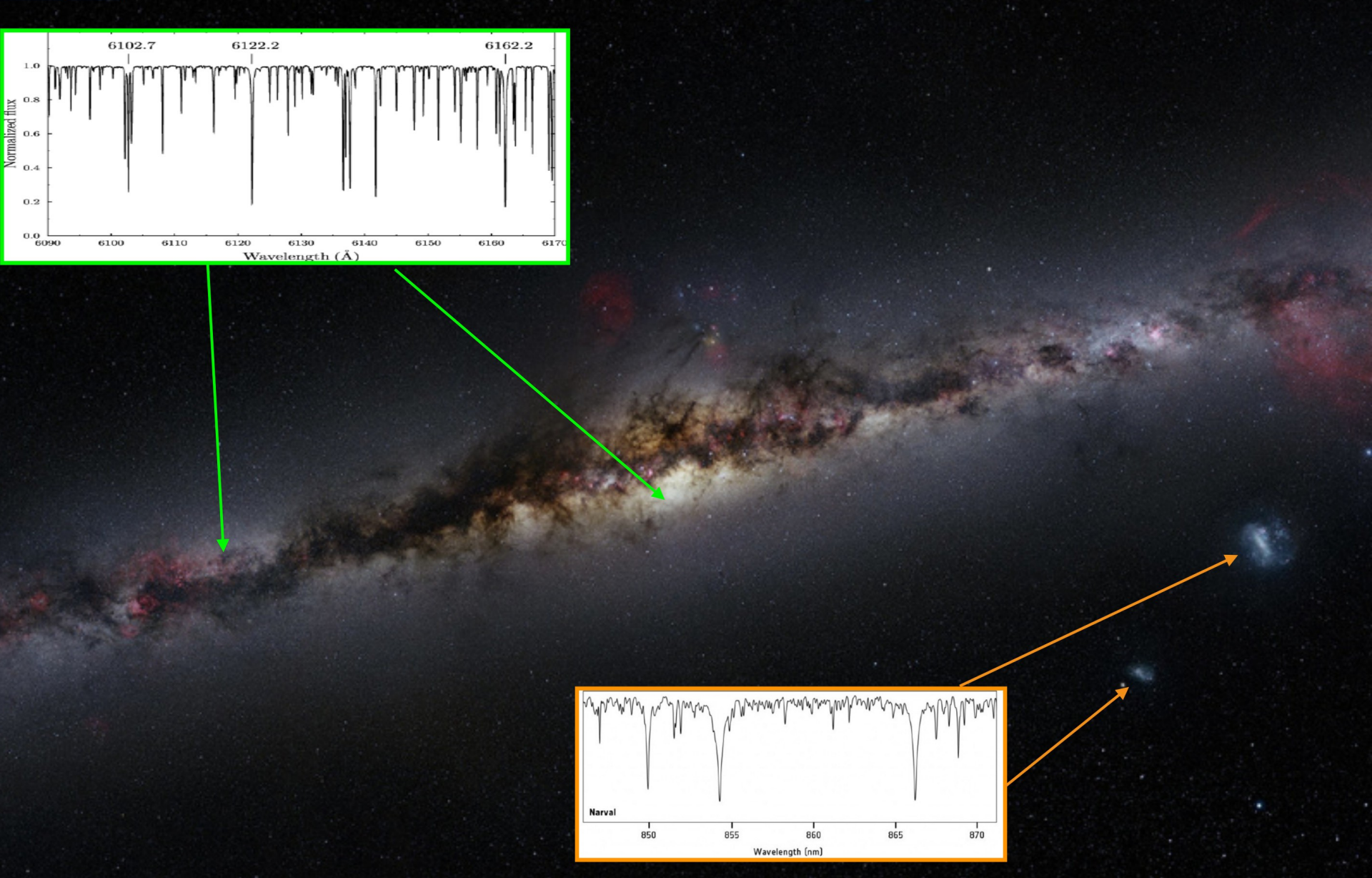
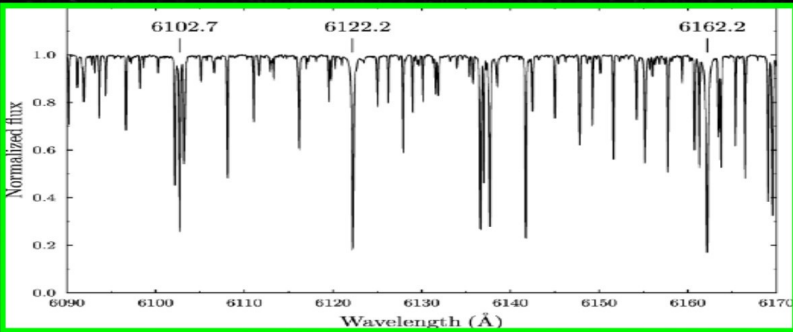
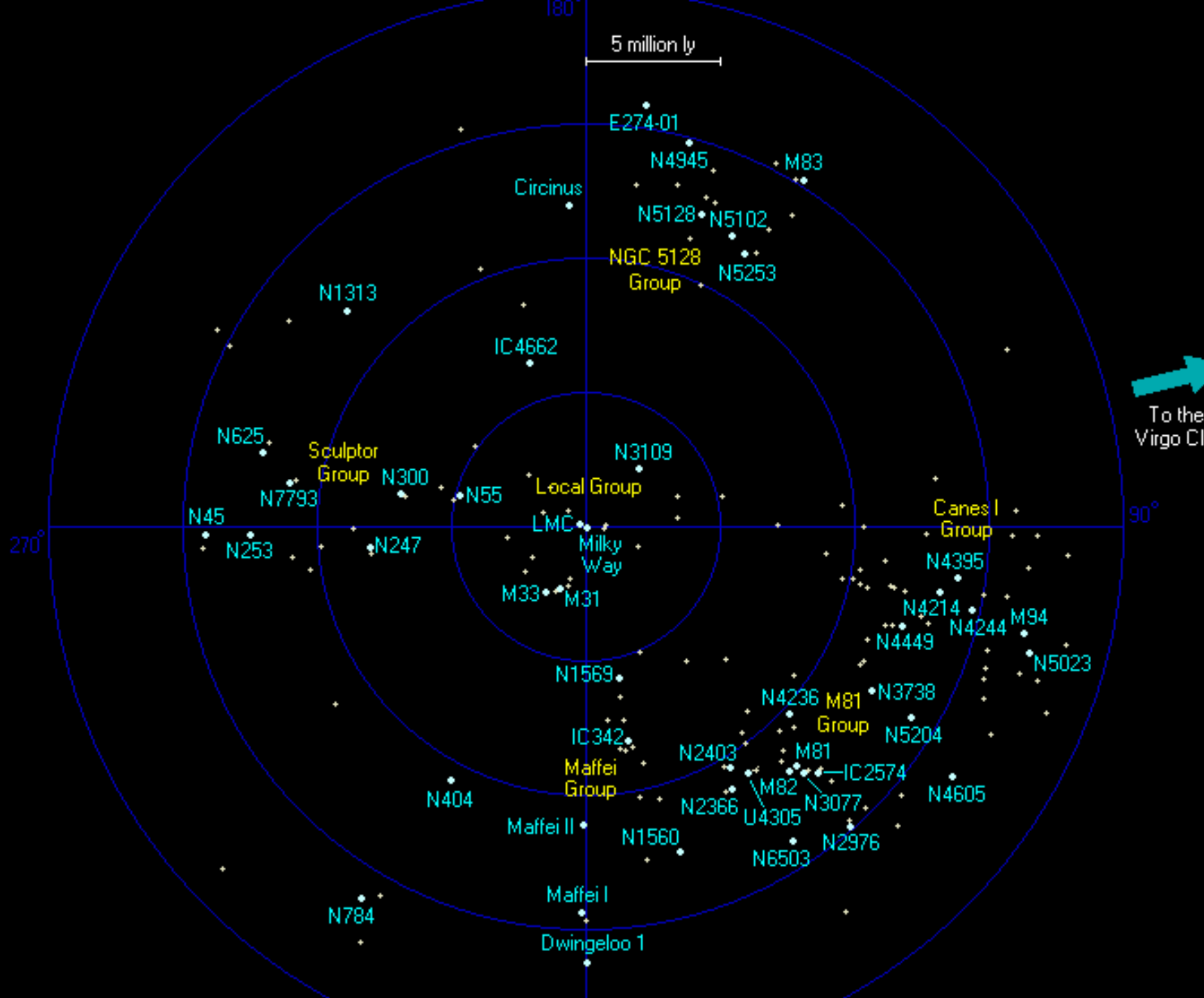


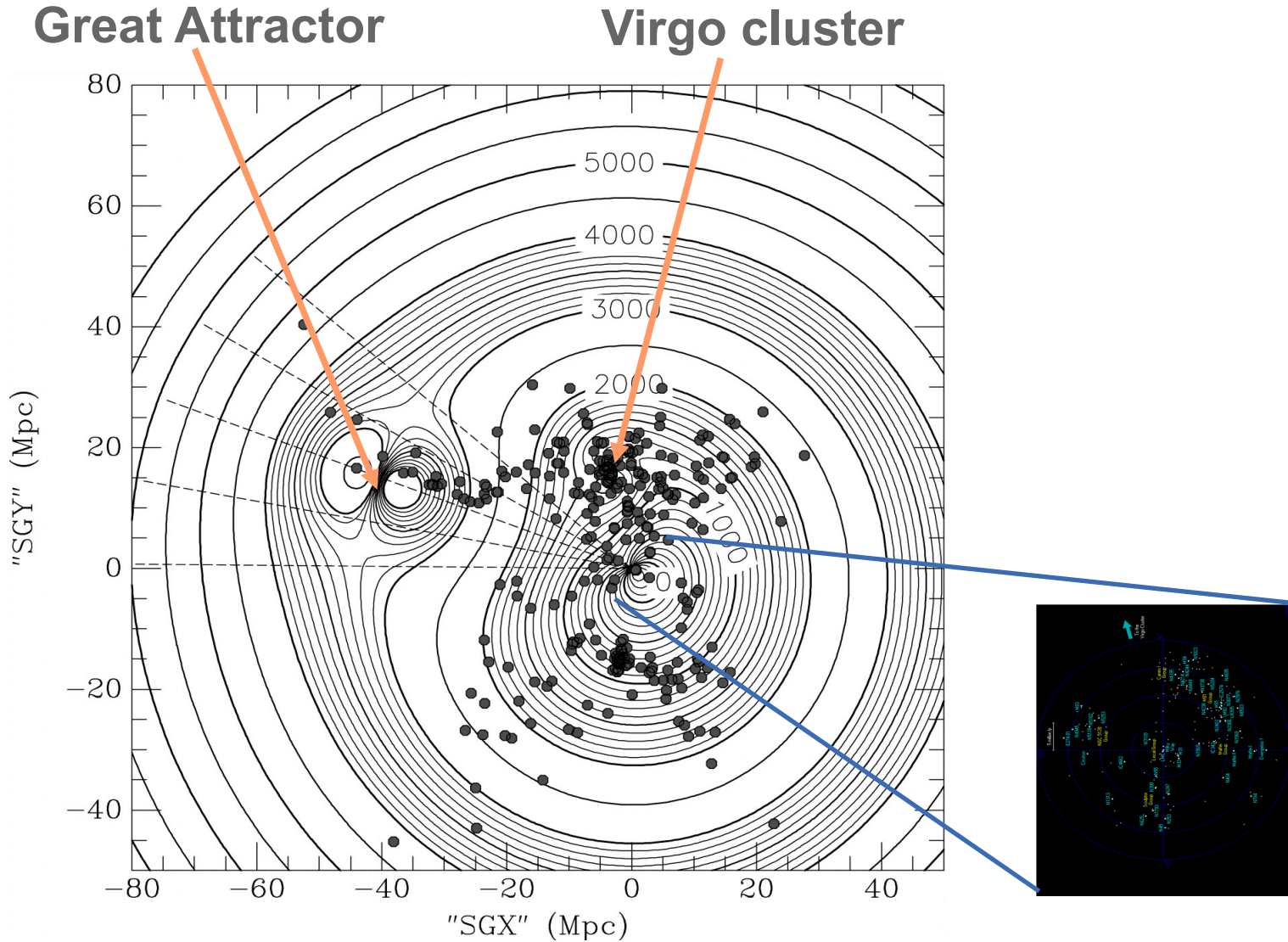


The Metallicity Ladder in Resolved Stellar Populations





Tonry et al. (2020)



Manu

1. Abundances for a single star (atmosphere etc.)
2. MDF of a CSP

Ivo

3. Outside of MWG, high-rez very difficult/time consuming except the nearest satellites
4. So switch to methods using lower-rez > CaT
5. to be interpreted with closed/open boxes

The Calcium triplet method

- ◆ Low-resolution spectroscopy of RGB stars in the CaII triplet region
- ◆ 2--4 AA FWHM
- ◆ $R \approx 2000\text{--}3000$
- ◆ Calibrated vs. stars with high-rez abundances

Pal 1=C0325+794

discovered by Abell (1955) on POSS plates
14 kpc from Sun
19 kpc from the GC
4.5 kpc above plane

$M_V = -2.5 \pm 0.5,$
 $M = 1300 \pm 600 M_{\text{sun}}$

HST horizon

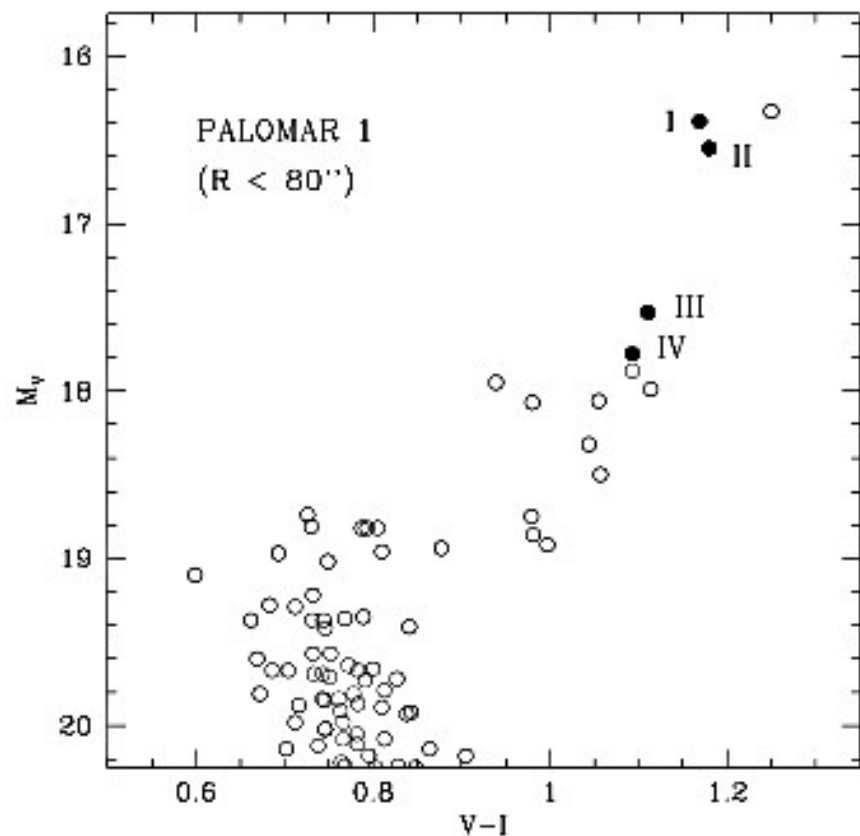


FIG. 1.— $V-I$ CMD of Pal 1. Only stars within the first $80''$ are represented. The upper part of the main sequence and the giant branch are clearly defined. Stars for which spectra have been obtained are identified by roman numerals.

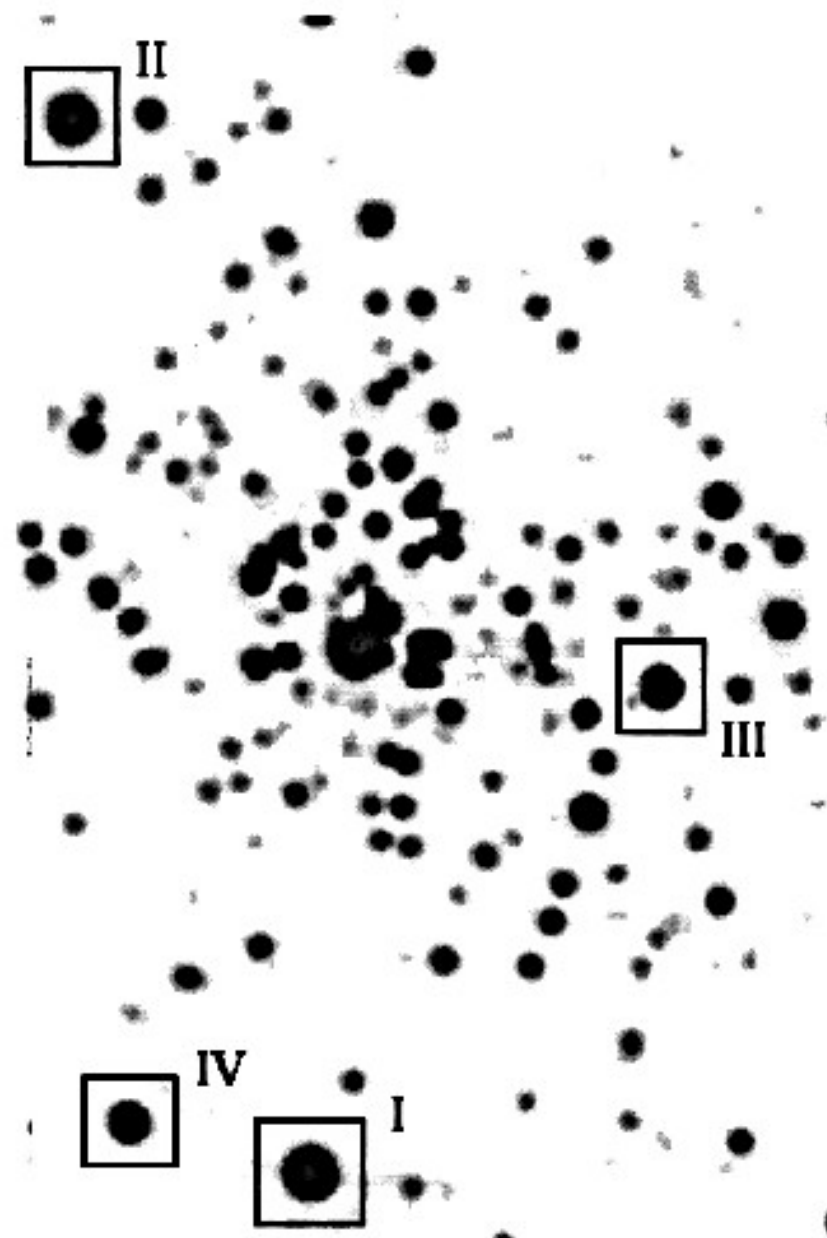


FIG. 2.—A 900 s I -band image of the central part of the cluster Pal 1 (1.4×1.5 , north up, west left). The stars for which spectra have been obtained are marked.

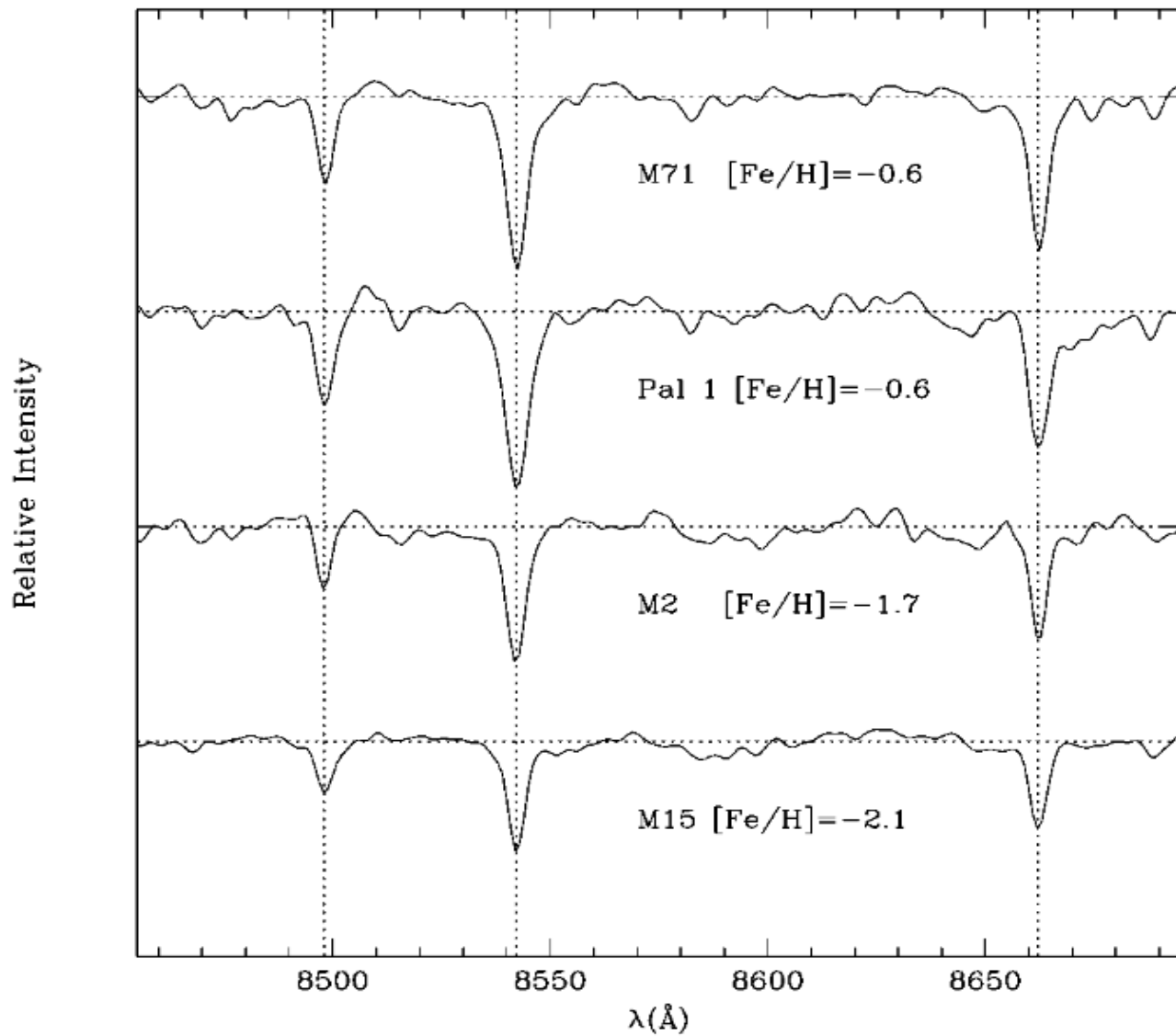


FIG. 3.—Sections of the spectra covering the Ca II triplet region for a single star of each observed cluster.

Definition of Equivalent Width

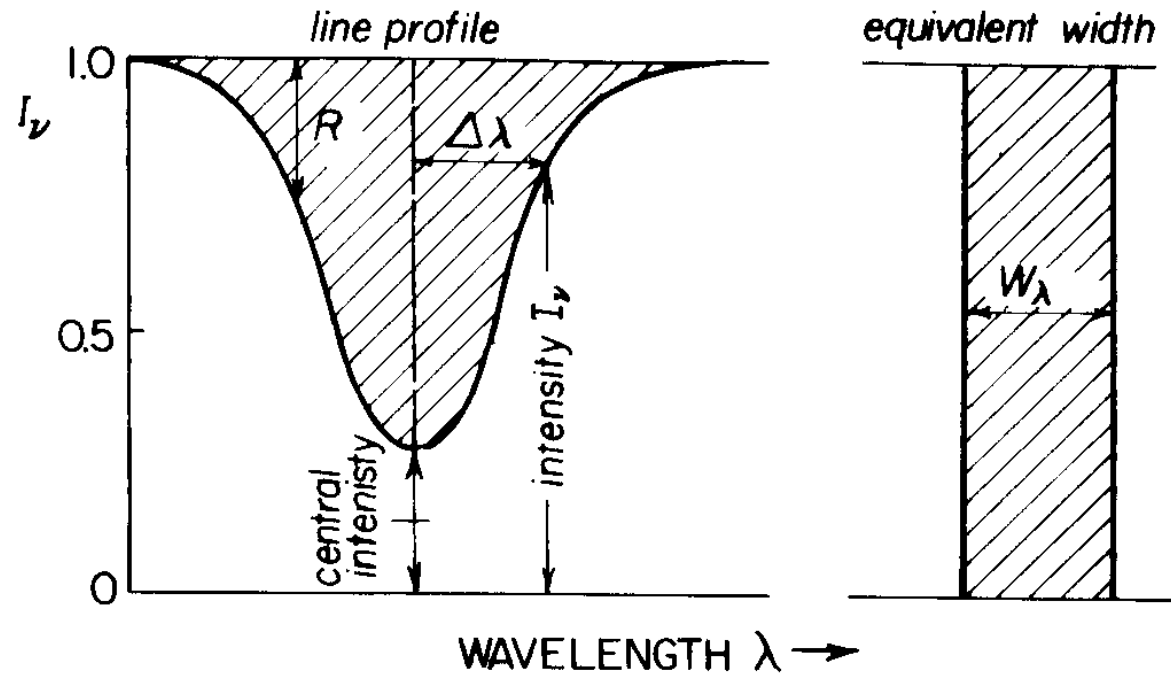


Fig. 3.4. Definition of equivalent width.

$$W_{\lambda} = \int R d\lambda$$

This measure becomes independent from flux units (units are Angstrom)

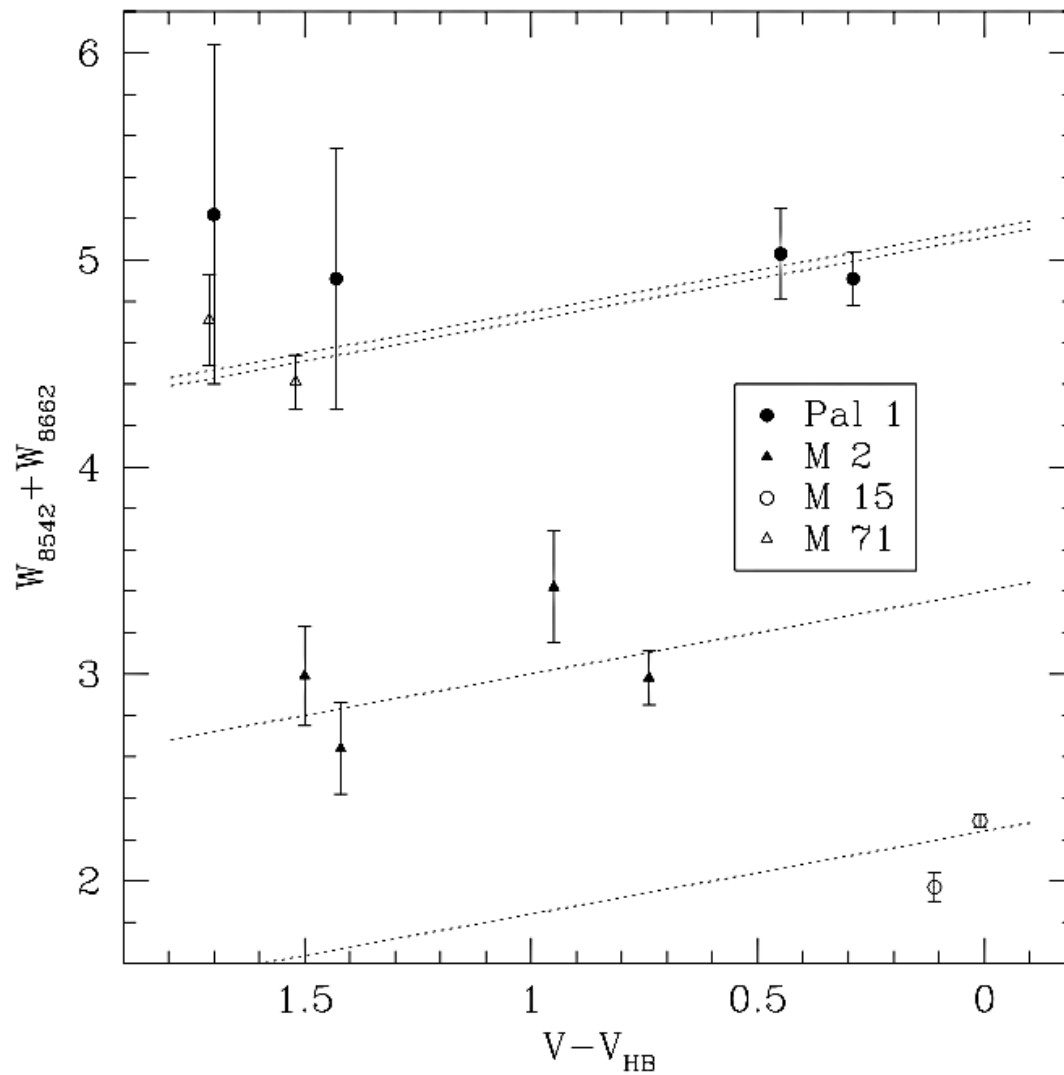


FIG. 4.—Summed equivalent widths and their associated errors plotted vs. $V - V_{HB}$ for the cluster member stars (including stars III and IV of M2). Dotted lines reproduce the adopted best fit, as described in the text.

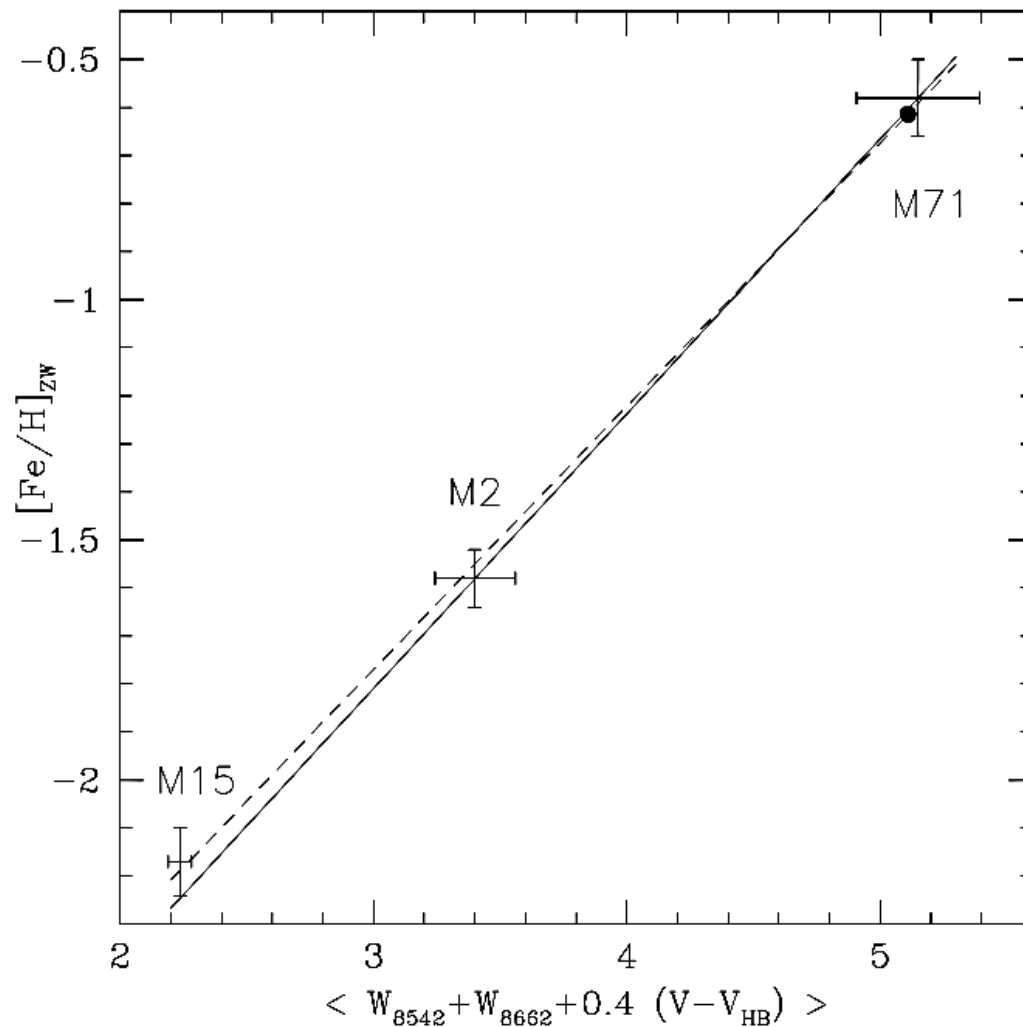


FIG. 5.—Abundance calibration for the Ca π line strengths. The reduced equivalent width W' is plotted against $[Fe/H]$ on the Zinn & West (1984) scale for the three calibration clusters. The dashed line was fitted to the three calibration points by least squares, while the solid line was fitted to M2 and M71. Both lines represent the adopted calibration relations.

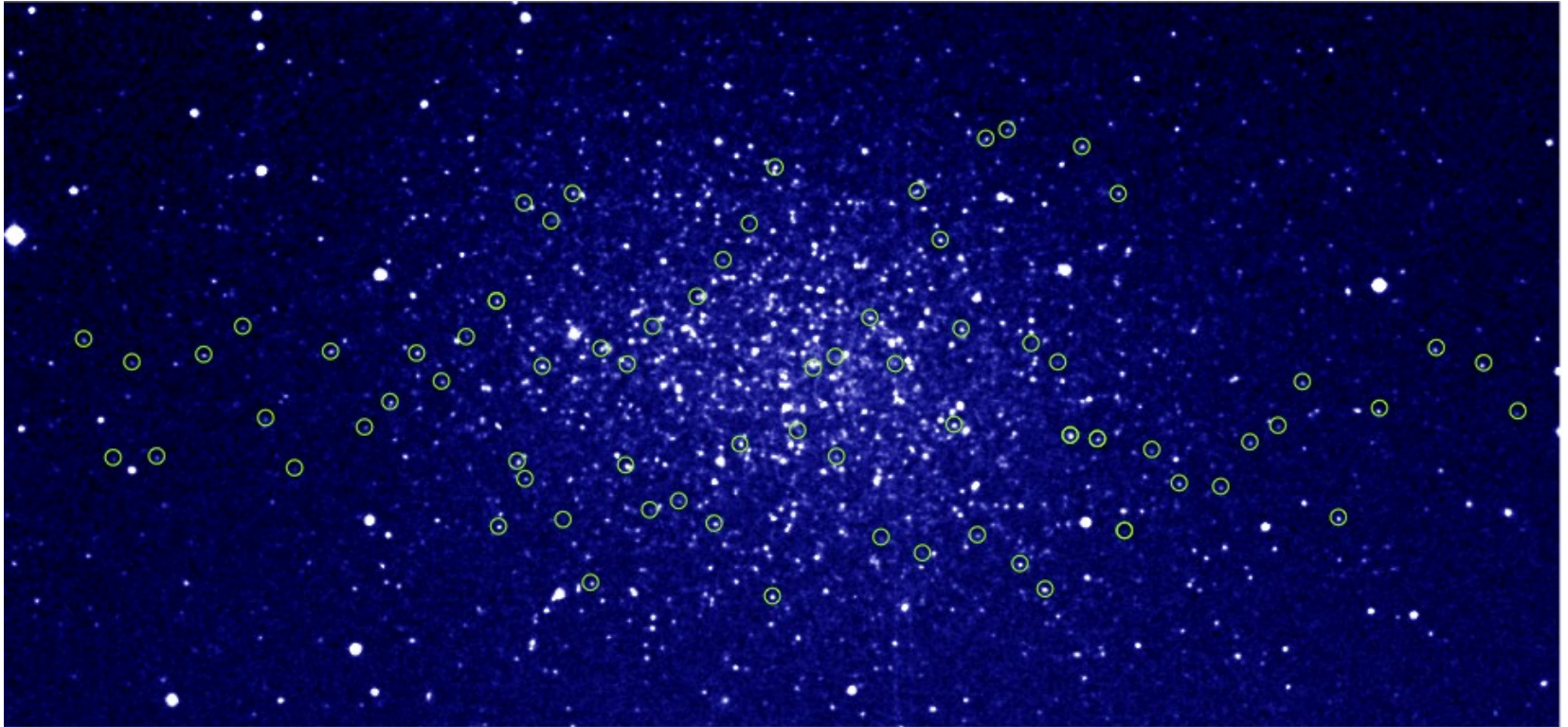
The Calcium triplet method

- ◆ Low-resolution spectroscopy of RGB stars in the CaI triplet region
- ◆ 2--4 AA FWHM
- ◆ $R \approx 2000\text{--}3000$
- ◆ Start with example of simple population

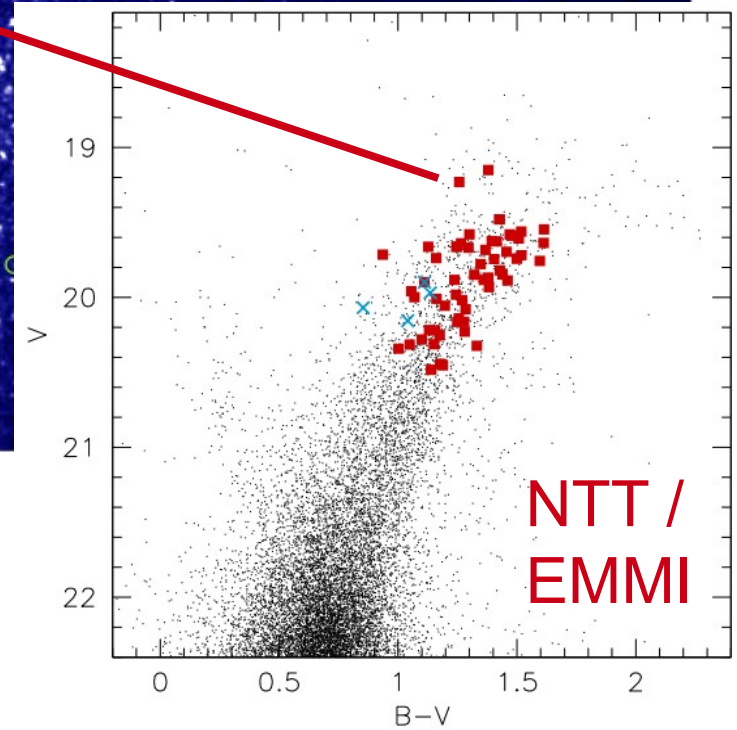
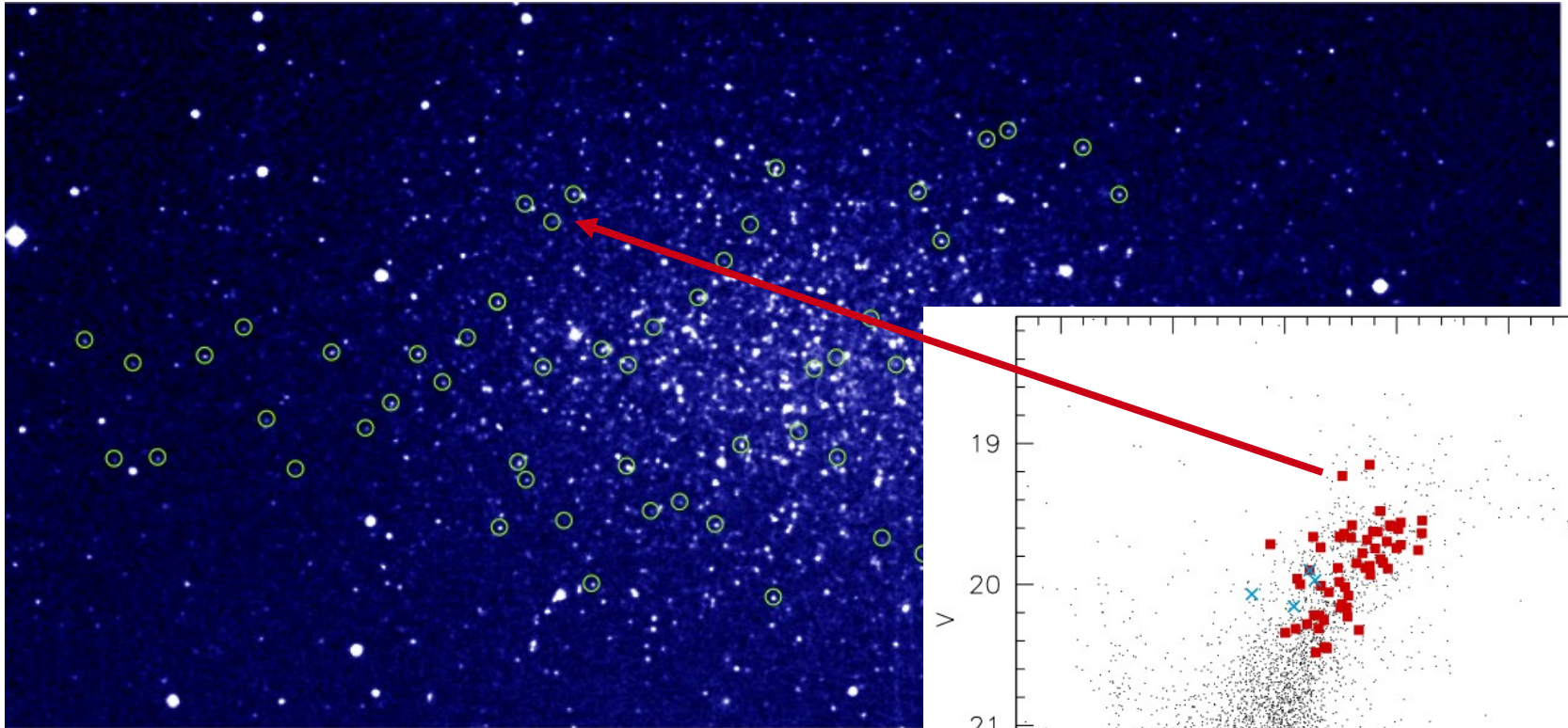
The Calcium triplet method

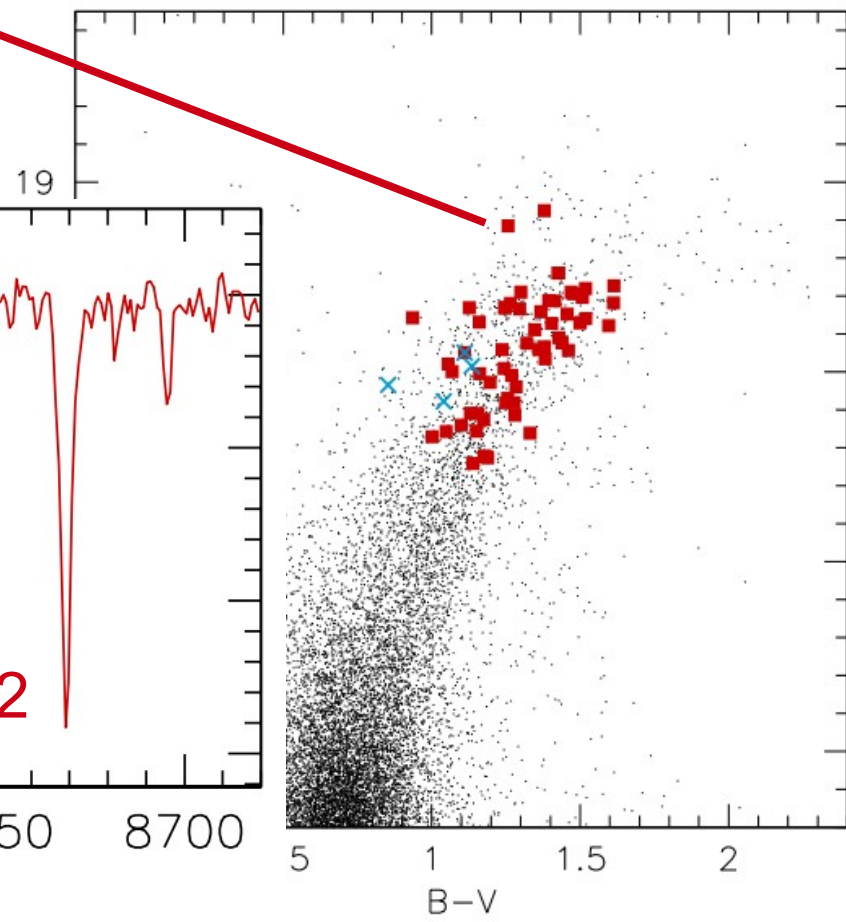
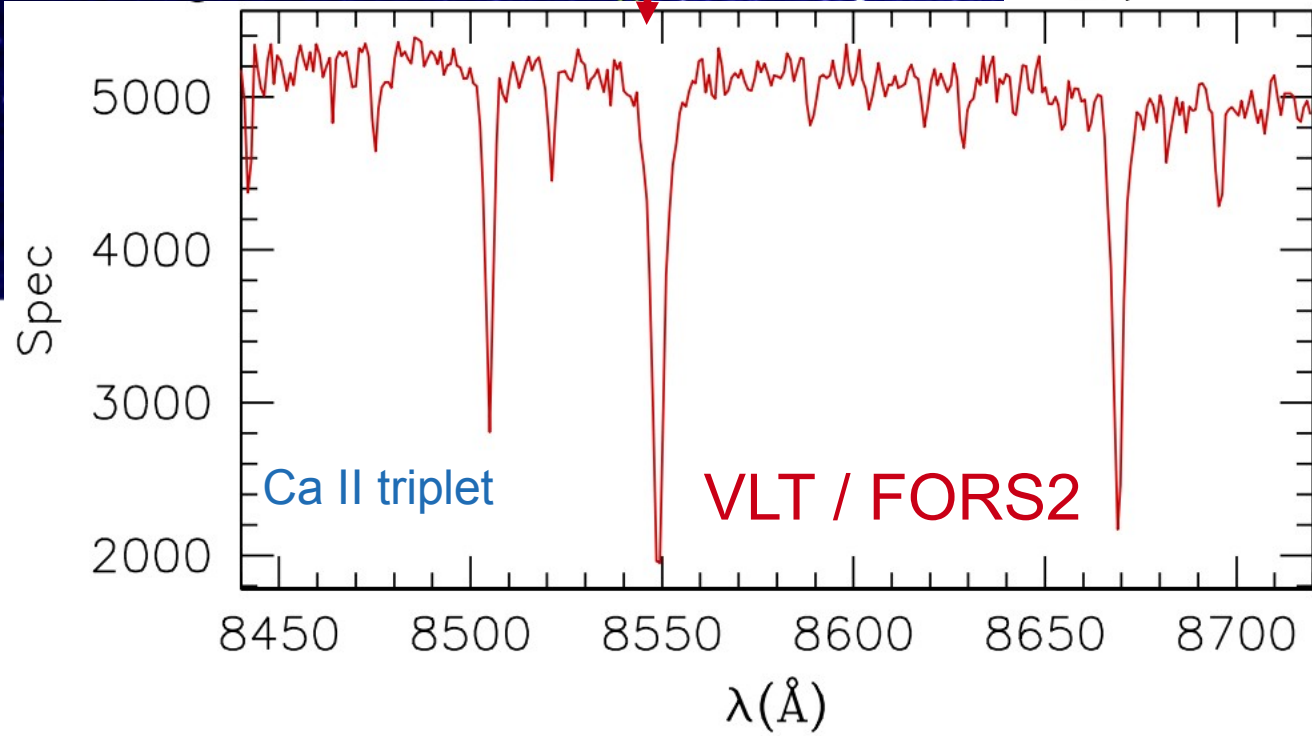
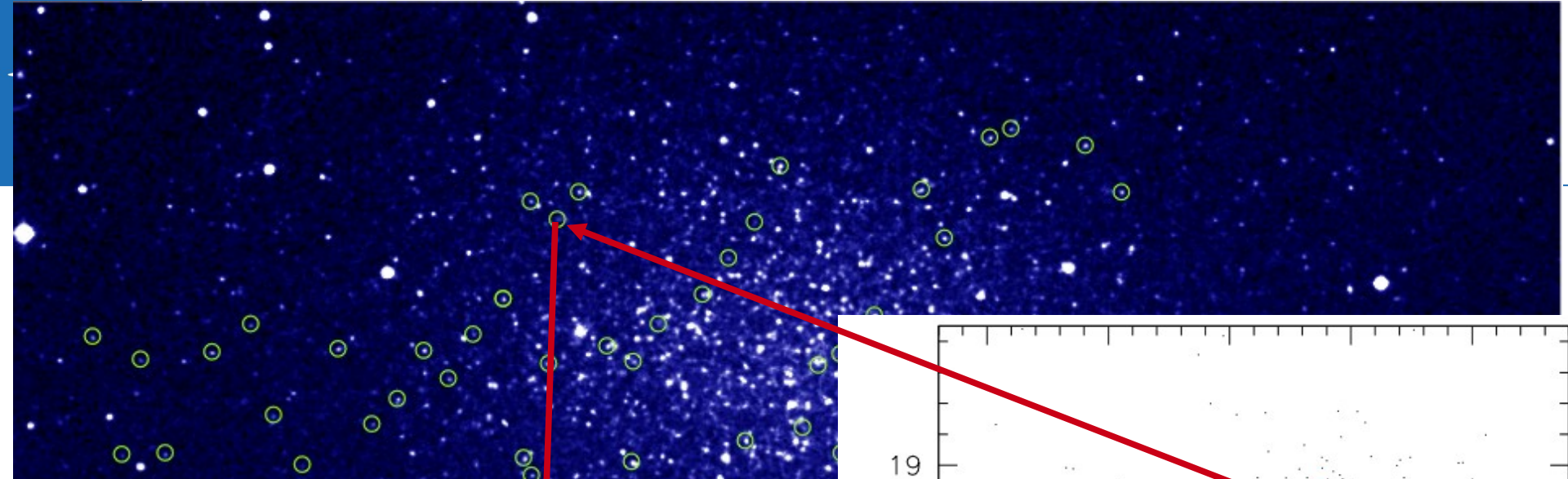
- ◆ Low-resolution spectroscopy of RGB stars in the CaII triplet region
- ◆ 2--4 AA FWHM
- ◆ $R \approx 2000\text{--}3000$
- ◆ Now try complex stellar population:
 - Leo I dwarf spheroidal galaxy

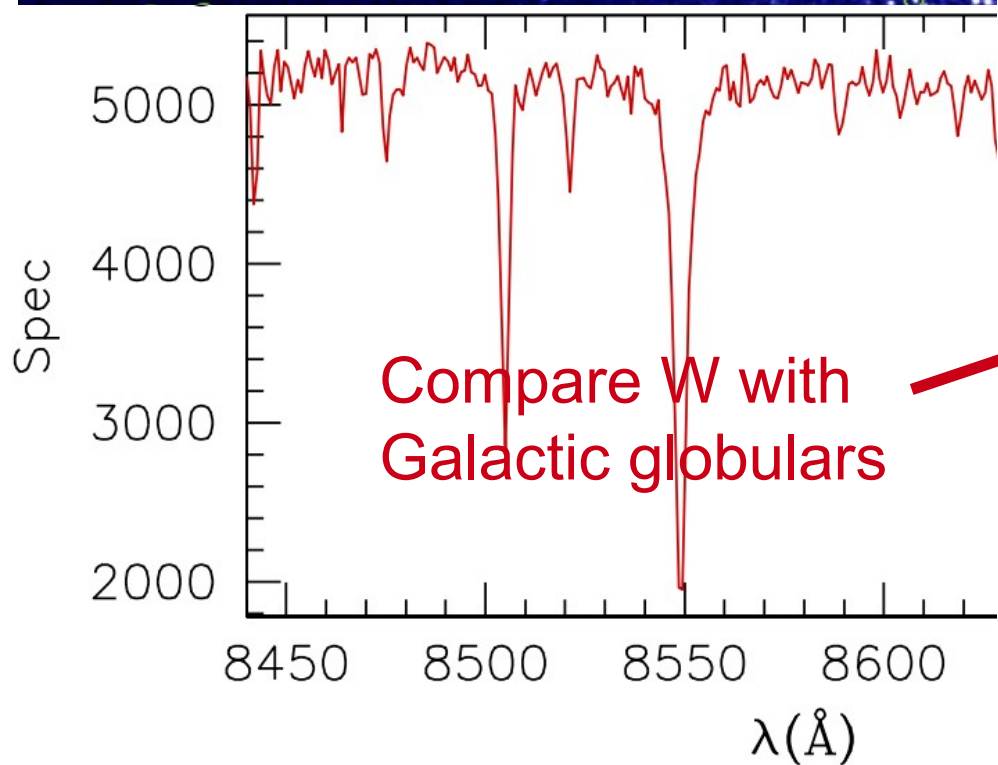
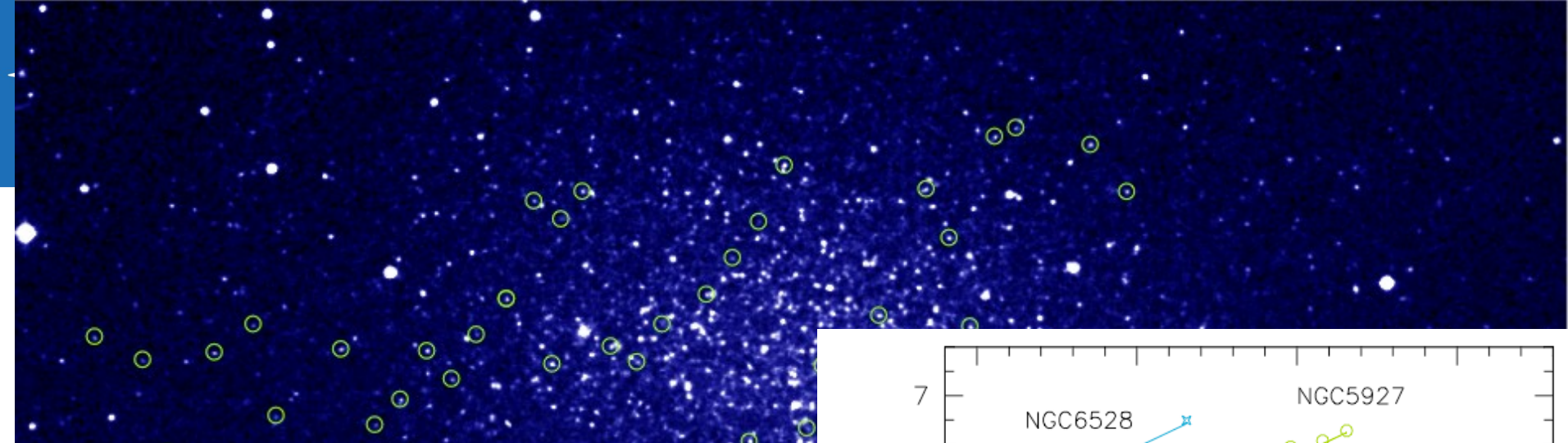
Leo I dwarf spheroidal galaxy



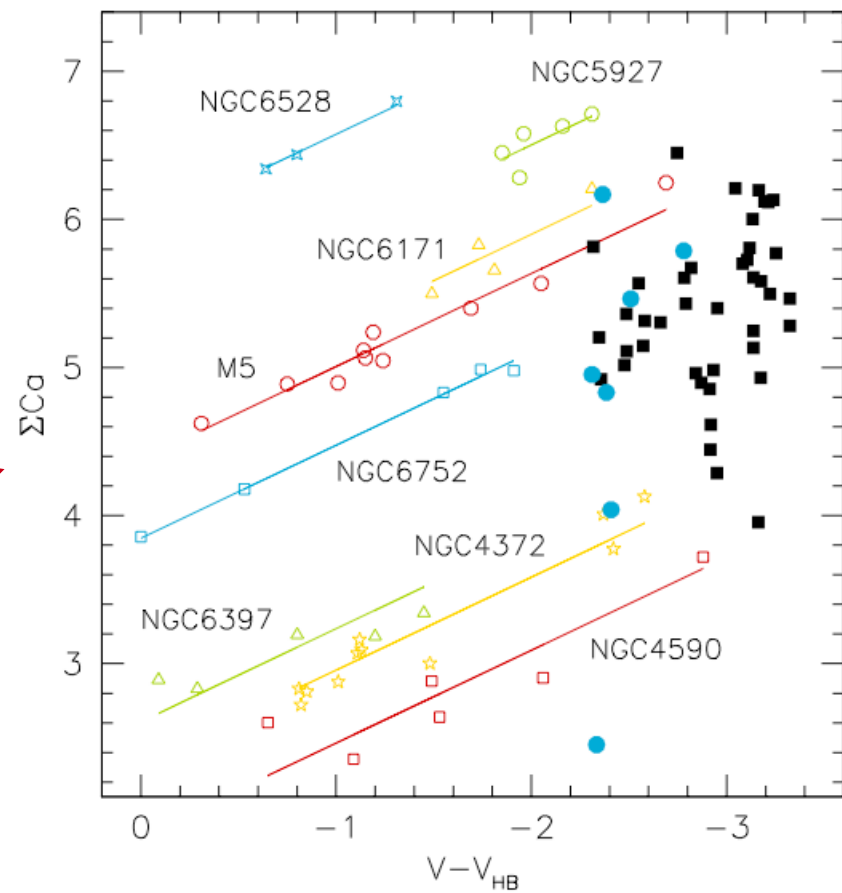
Leo I dwarf spheroidal galaxy







Compare W with
Galactic globulars



Simple vs. complex

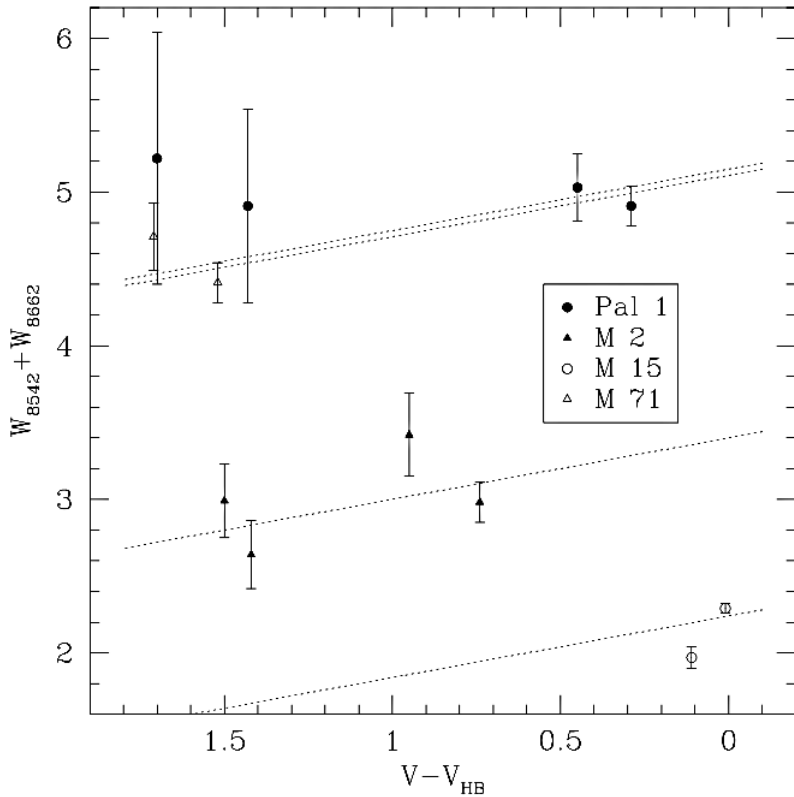
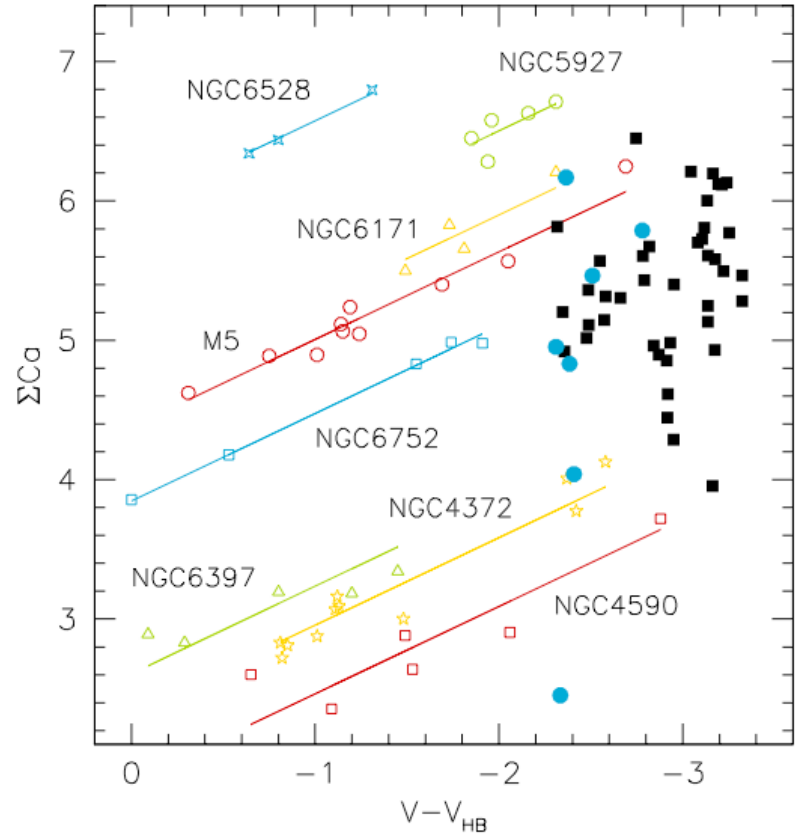


FIG. 4.—Summed equivalent widths and their associated errors plotted vs. $V - V_{HB}$ for the cluster member stars (including stars III and IV of M2). Dotted lines reproduce the adopted best fit, as described in the text.



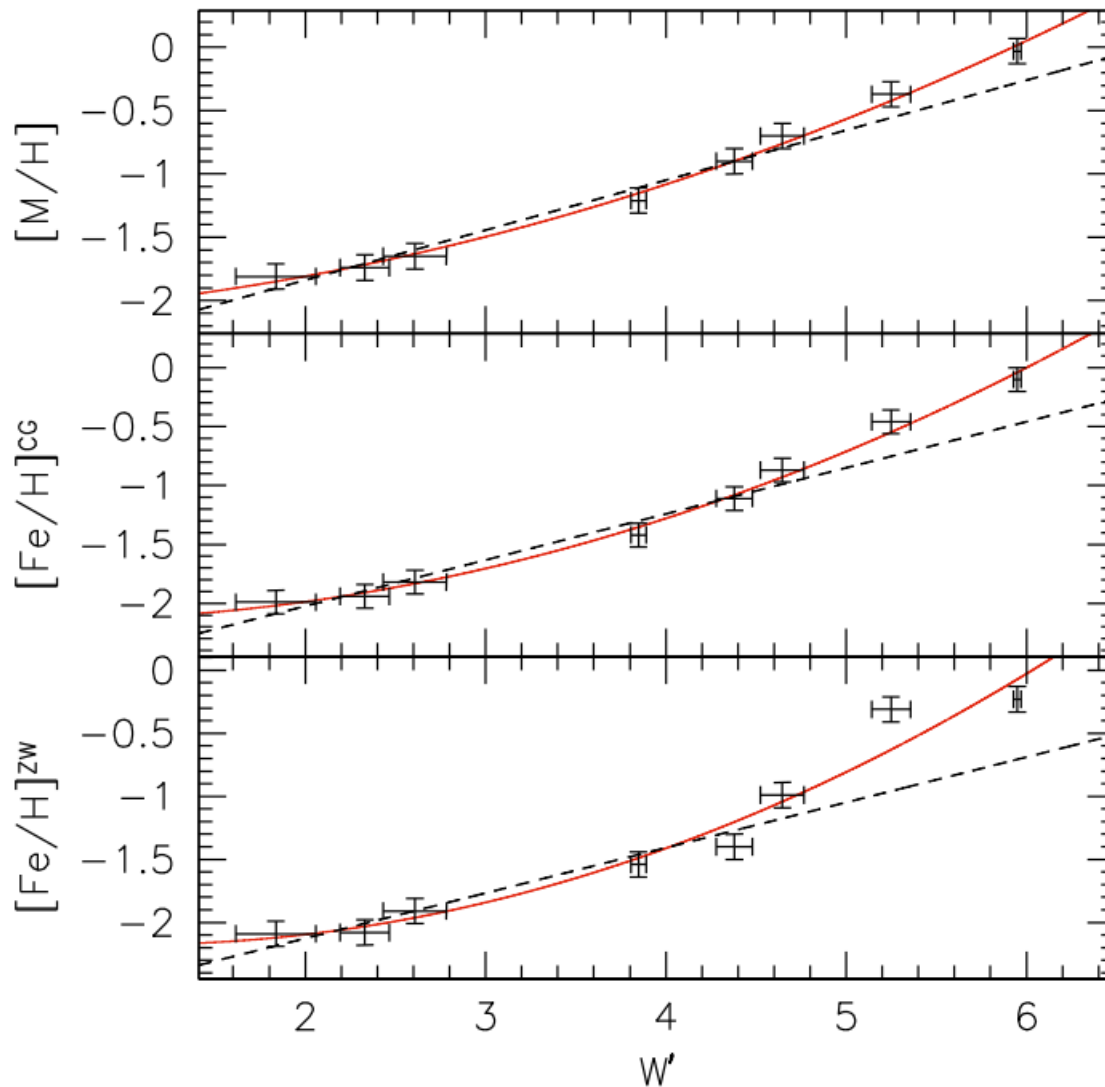


Fig. 7. The metallicity of the reference globular clusters against the reduced EW of CaT lines, for three adopted metallicity scales. The *solid* lines are quadratic fits, while the *dashed* straight lines are linear fits obtained for clusters with $[Fe/H] < -0.6$.

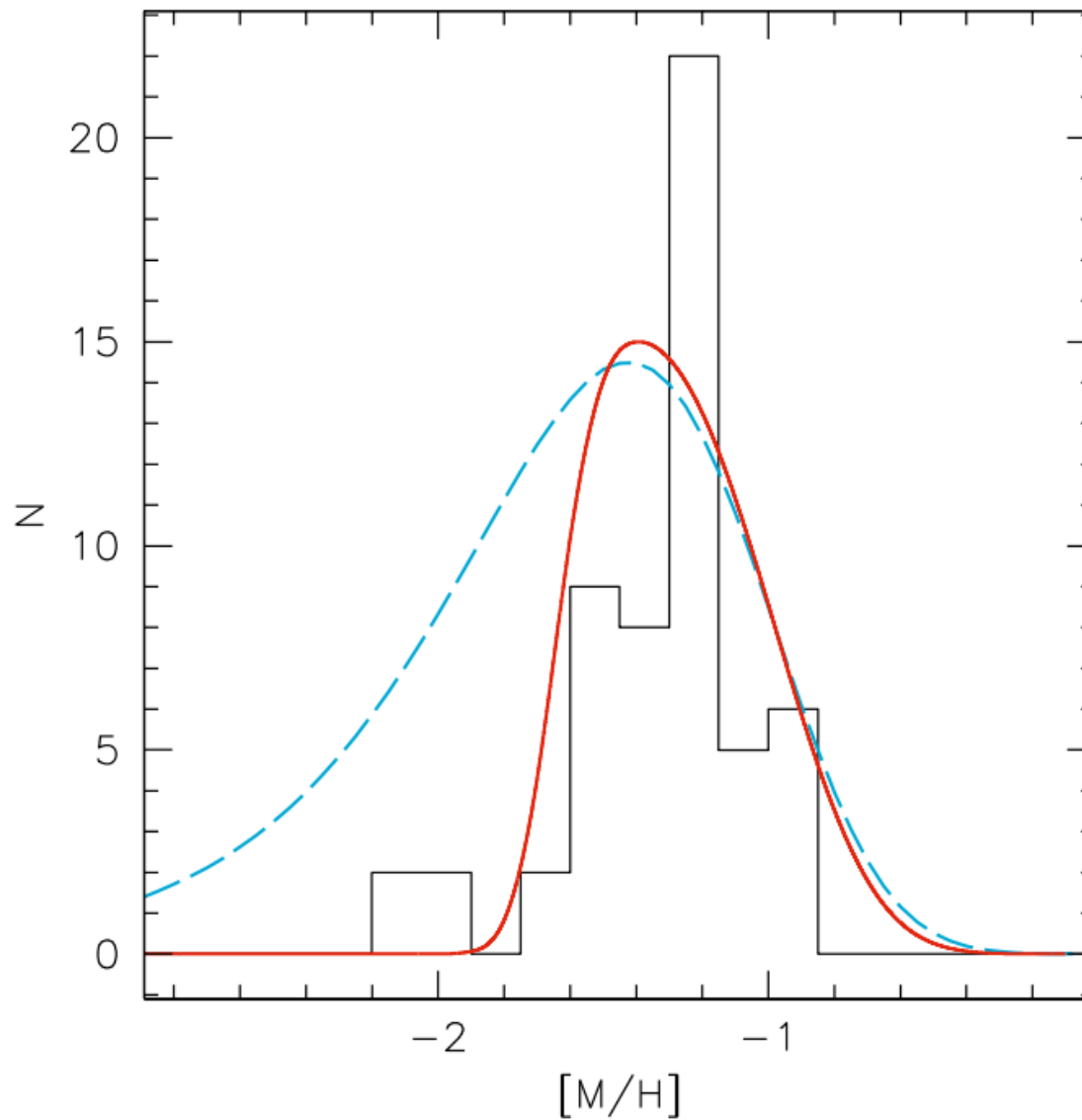


Fig. 9. The MDF of Leo I RGB stars on the $[M/H]$ metallicity scale, compared with a simple model with a low effective yield (*dashed line*) and a model with a prompt initial enrichment (*solid line*).

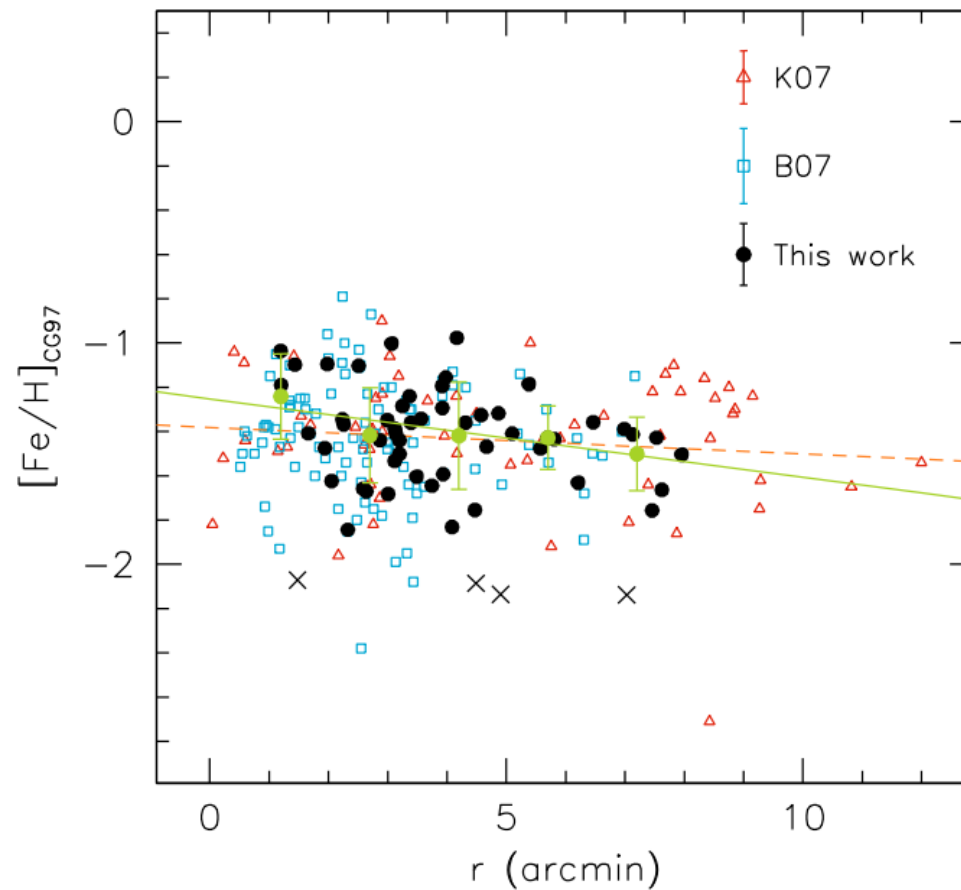


Fig. 10. Metallicities of Leo I stars on the $[\text{Fe}/\text{H}]$ scale of CG97, plotted against the elliptical radius (see text). *Filled dots*: data in this paper; *open squares*: data from Bosler et al. (2007); *open triangles*: Koch et al. (2007b); *circles with error bars*: our data, binned in 1'.5 bins. The error bars of the binned data represent the abundance scatter (1σ) in each bin. The *crosses* are the 4 metal-poor stars in our sample. The typical errors of each study are shown in the upper right corner of the plot. The *solid line* is a fit to our (binned) data, while the *dashed line* represents a fit to all available spectroscopic data.

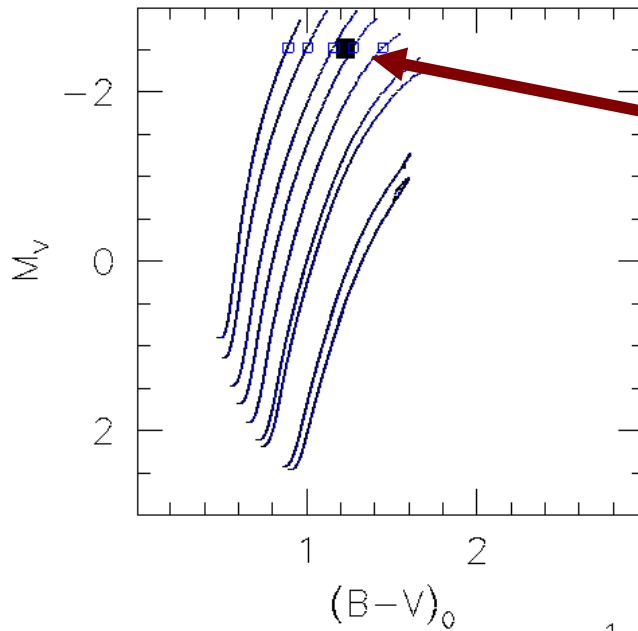
With:

- color
- luminosity
- metallicity

+ some isochrone interpolation
machinery by Ivo...

=> **age** of each star

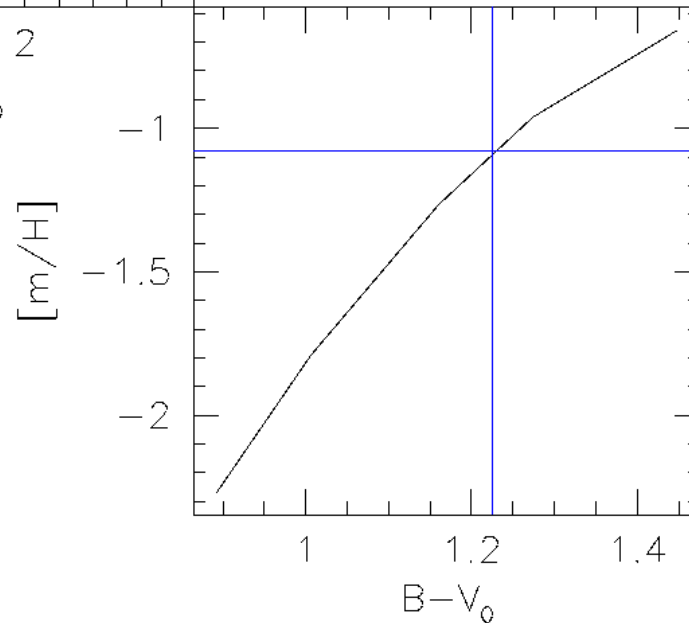
For each age..



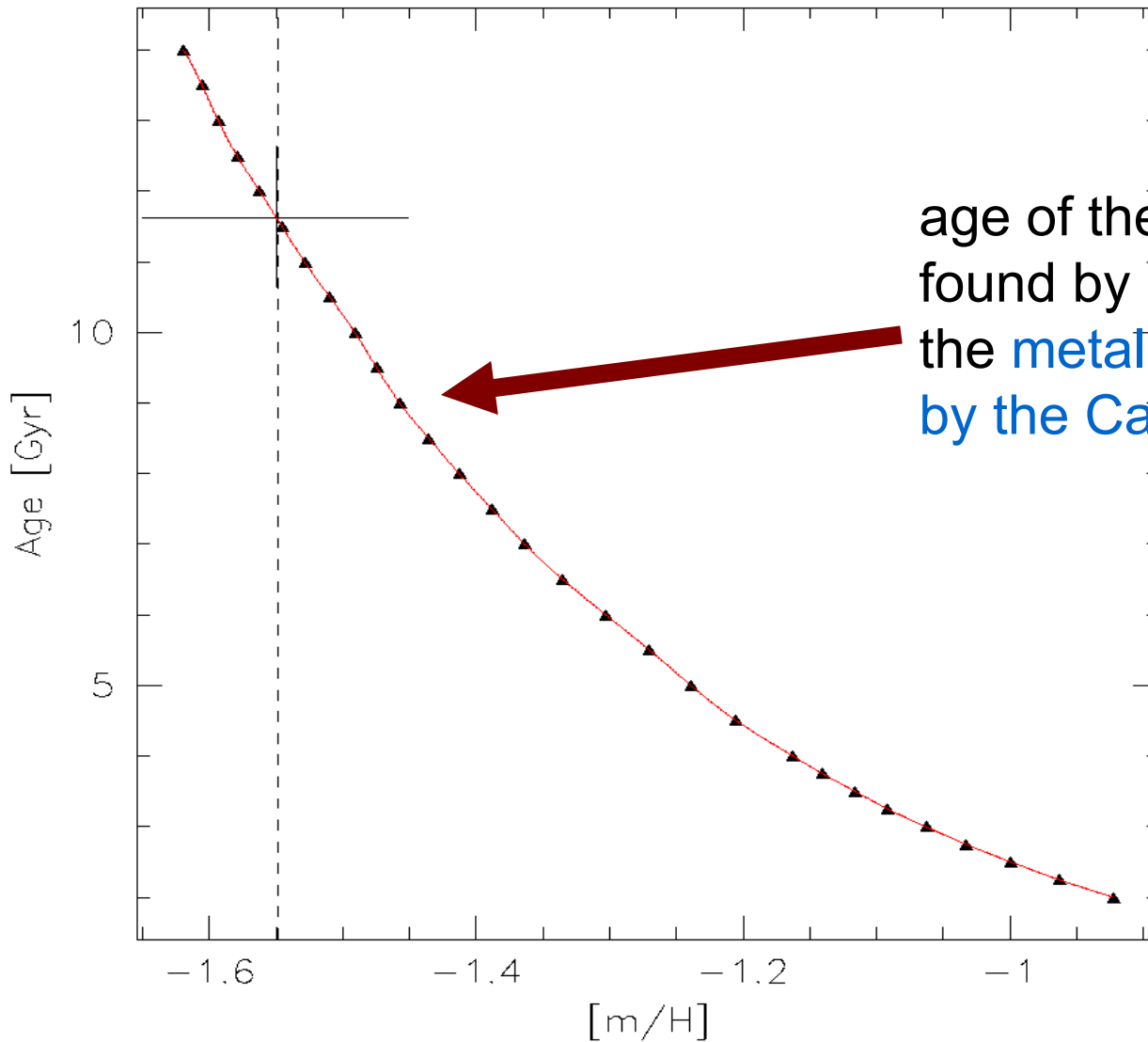
Find isochrone's color of RGB at luminosity of each star

Metallicity-color relation interpolated by a cubic spline

=> compute metallicity at stars' color



Then **change age** and repeat => age vs. [m/H]



age of the star can be found by using the **metallicity yielded by the CaT method**

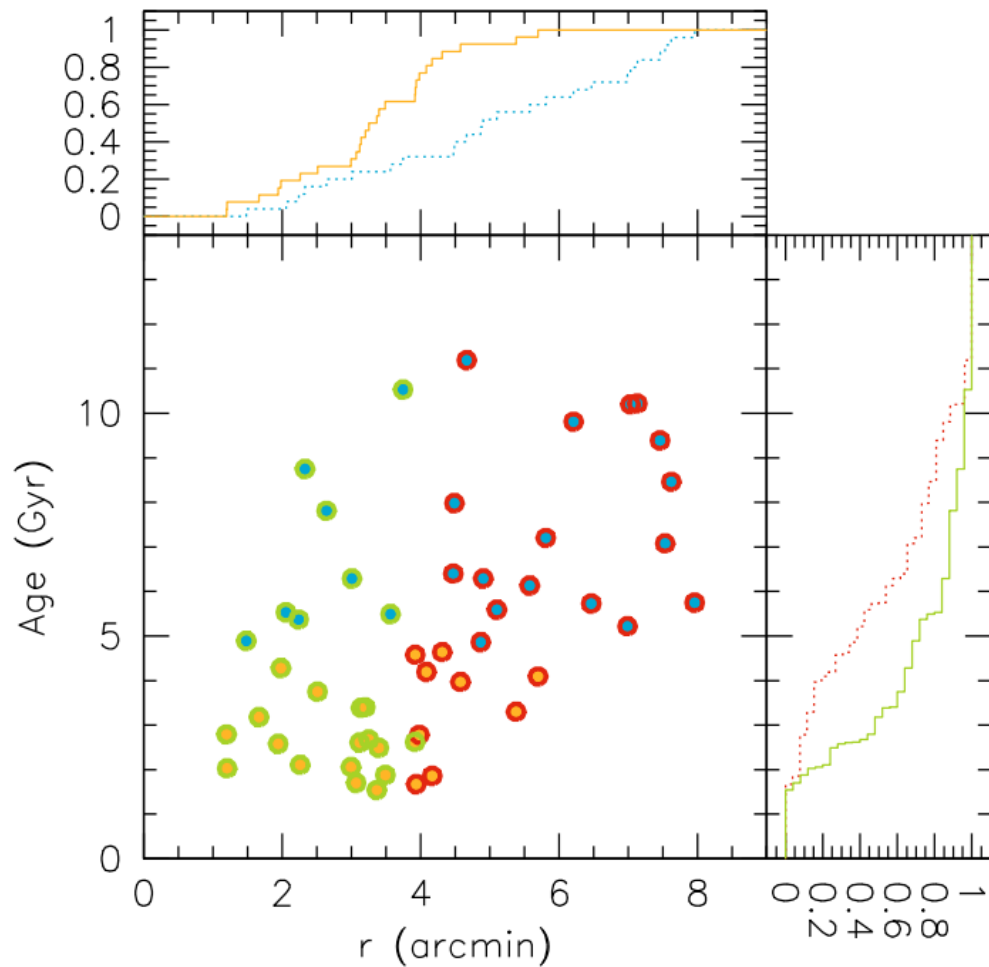


Fig. 12. Ages of the Leo I stars in our sample as a function of the elliptical radius (*central panel*). The *upper panel* shows the cumulative radial distributions of stars with ages smaller and larger (dotted line) than 4.6 Gyr. The cumulative age distributions of stars in the inner ($r < 3.9$) and outer ($r > 3.9$, dotted line) region are shown in the *right panel* (the different age and radial intervals are colour-coded in the electronic version of the journal). Younger stars appear to be more concentrated towards the centre of Leo I.

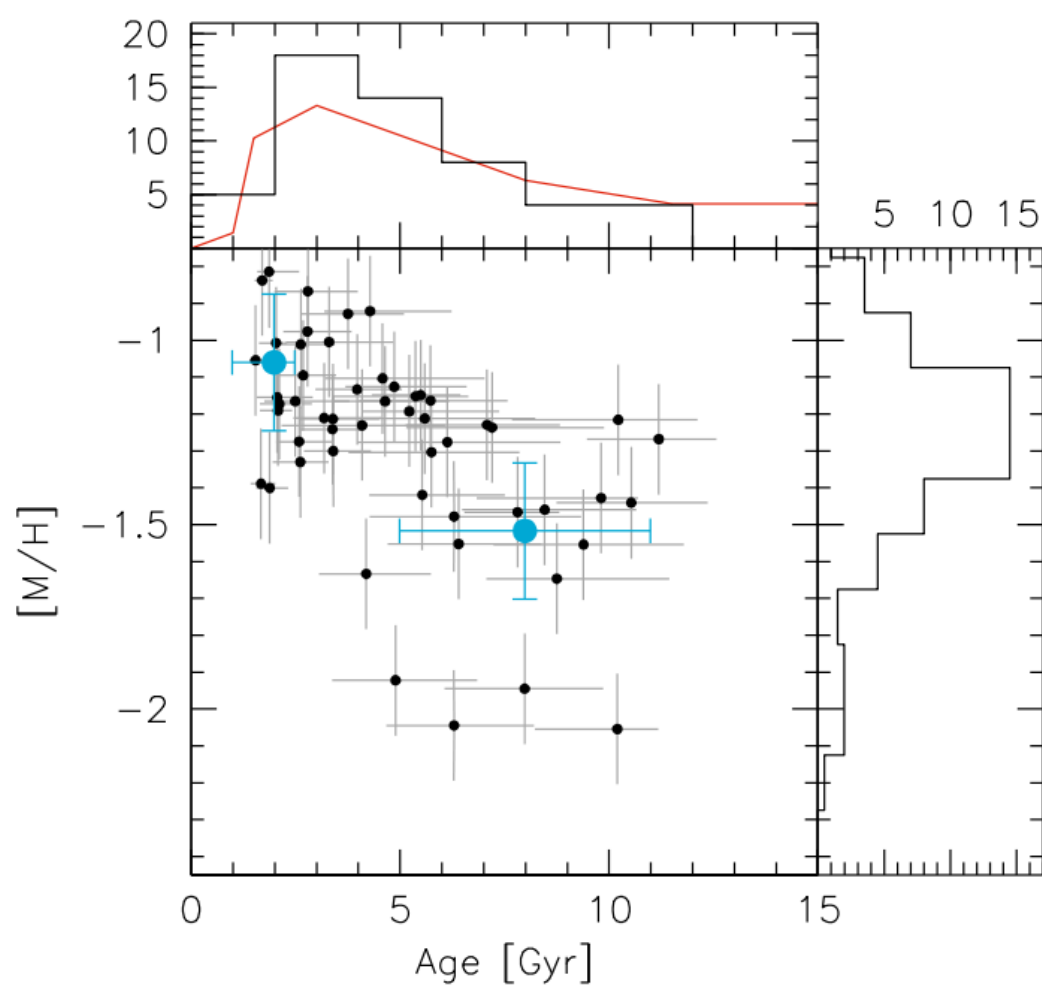
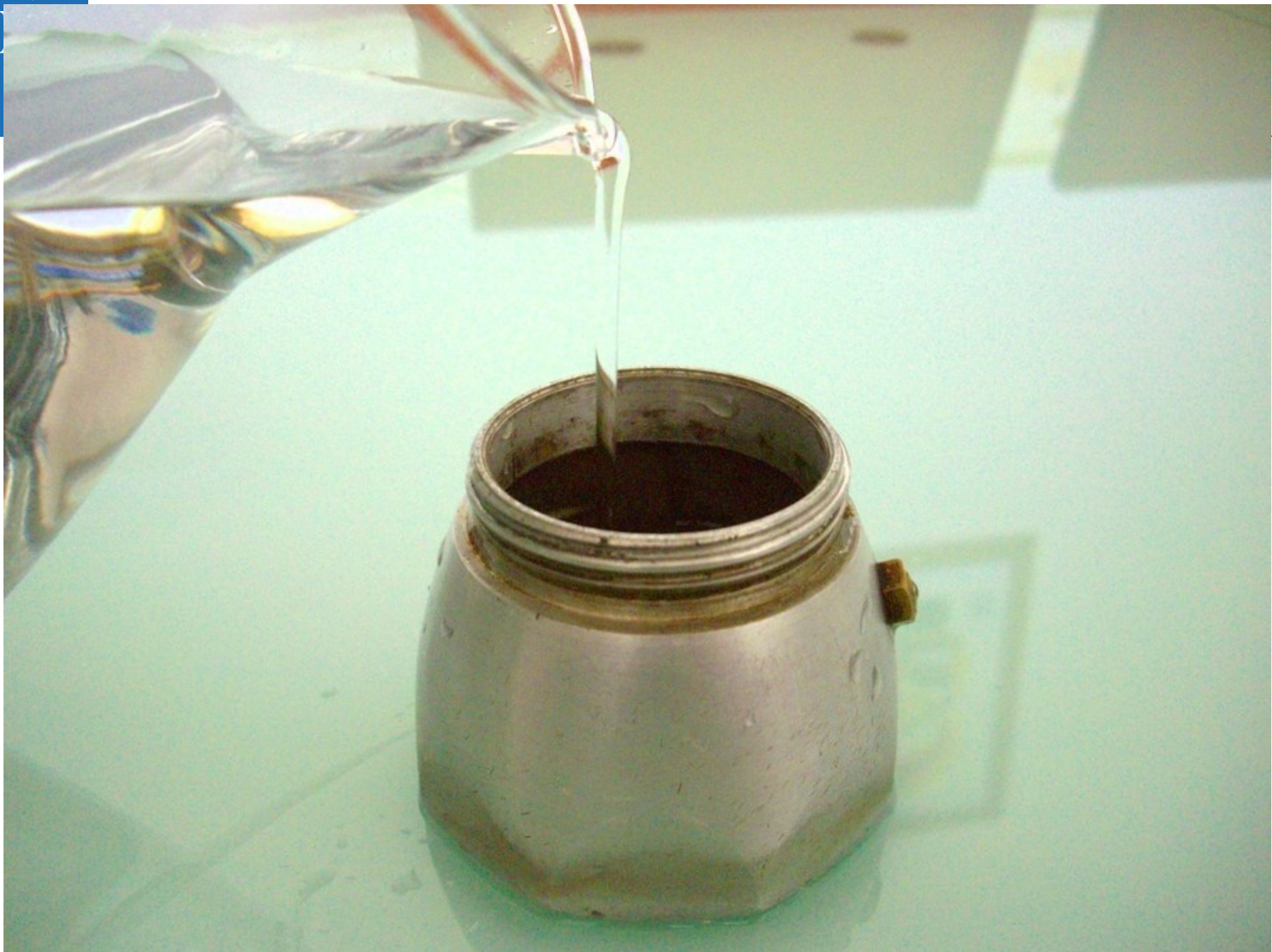


Fig. 11. The age-metallicity relation of Leo I RGB stars in our sample, on the $[M/H]$ scale. The error bars in age represent the first and third quartile of the confidence intervals obtained through Monte Carlo realisations (see text for details). For the metallicity errors the representative value discussed in Sect. 4.3 is adopted. Also shown are the metallicities from high-resolution spectroscopy of two Leo I RGB stars from Tolstoy et al. (2003) (*big filled circles*). The side histograms are the marginal distributions in metallicity and age. The *solid line* in the *top panel* represents the SFH derived by Dolphin (2002) from HST photometry, normalised to the total number of stars in our sample.

The closed box model













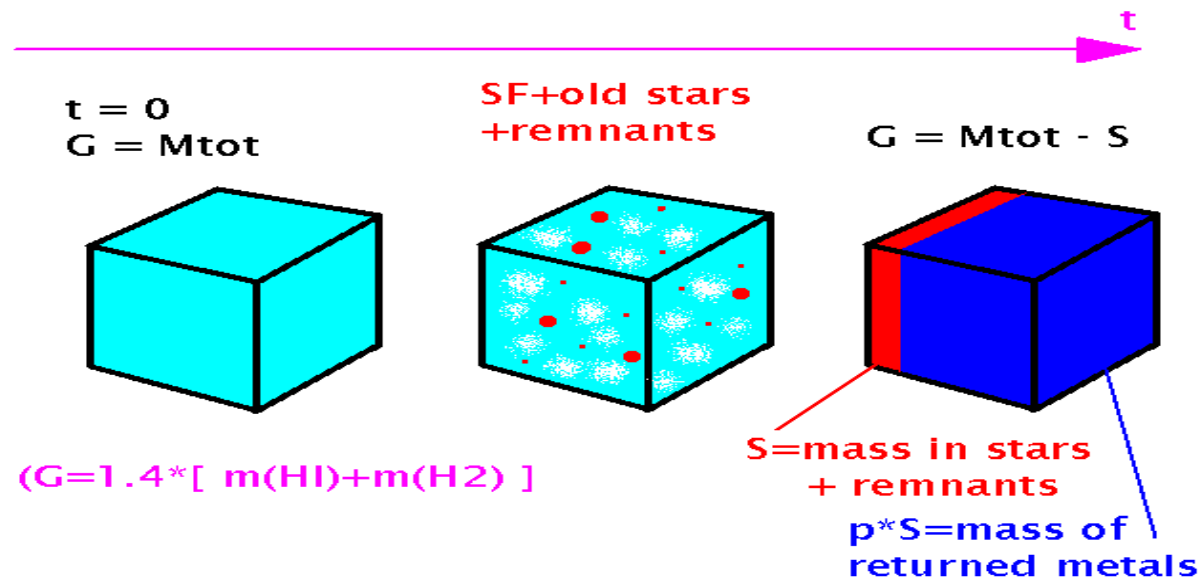








The "simple model" of GCE



Isolated system

Perfect mixing

IMF = const

Nucleosynthetic yields $p = \text{const}$

Instantaneous recycling (e.g. Oxygen)

"real" models => relax one or more hypothesis (e.g. Delayed formation for N)

$$p_i = \frac{\int_{m(t)}^{m_U} m q_i(m) \phi(m) dm}{S}$$

Yield per stellar mass

IMF



$$Z = \frac{M_Z}{G} = \frac{pS}{G}$$

$$Z + dZ = \frac{M_Z + p dS}{G}$$

$$Z + dZ = Z + p \frac{dS}{G}$$

$$dZ = p \frac{-d(M_{\text{tot}} - S)}{G}$$

$$dZ = -p \frac{dG}{G}$$

$$Z_1 - Z_0 = -p \ln \frac{G_1}{G_0}$$

$$Z = -p \ln \frac{1}{\mu}$$

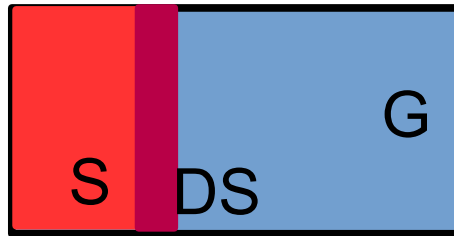
$$[Z_0 = 0; Z_1 = Z$$

$$G_0 = M_{\text{tot}}; G_1 = G$$

$$\mu = \frac{G}{M_{\text{tot}}}]$$

Basic equations

$$M_{\text{tot}} = G + S \Rightarrow dG = -dS$$



$$dZ = p \frac{dS}{G}$$

$$\frac{dS}{dZ} = \frac{1}{p} G$$

$$\bar{m} \frac{dN}{dZ} = \frac{1}{p} G$$

$$\bar{m} \frac{dN}{dZ} = \frac{1}{p} M_{\text{tot}} e^{-Z/p}$$

$$\frac{dN}{dZ} = \frac{M_{\text{tot}}}{\bar{m}} \frac{1}{p} e^{-Z/p}$$

Metallicity of
ISM

Metallicity of
stars



$$M_{\text{tot}} = M^* + M_{\text{gas}} = \text{constant}$$

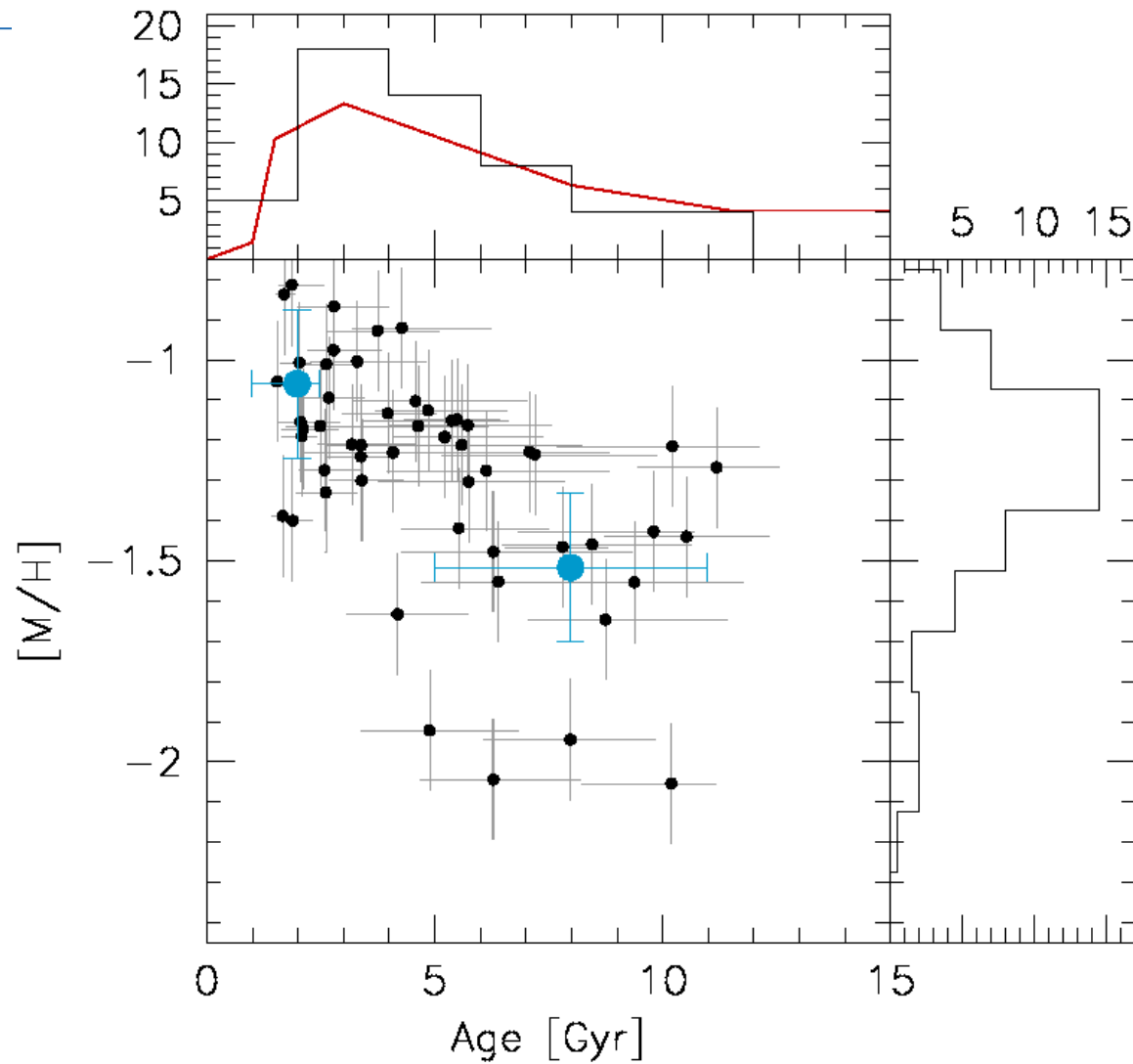
$$\mu = M_{\text{gas}} / M_{\text{tot}}$$

$$Z = p \ln \frac{1}{\mu}$$

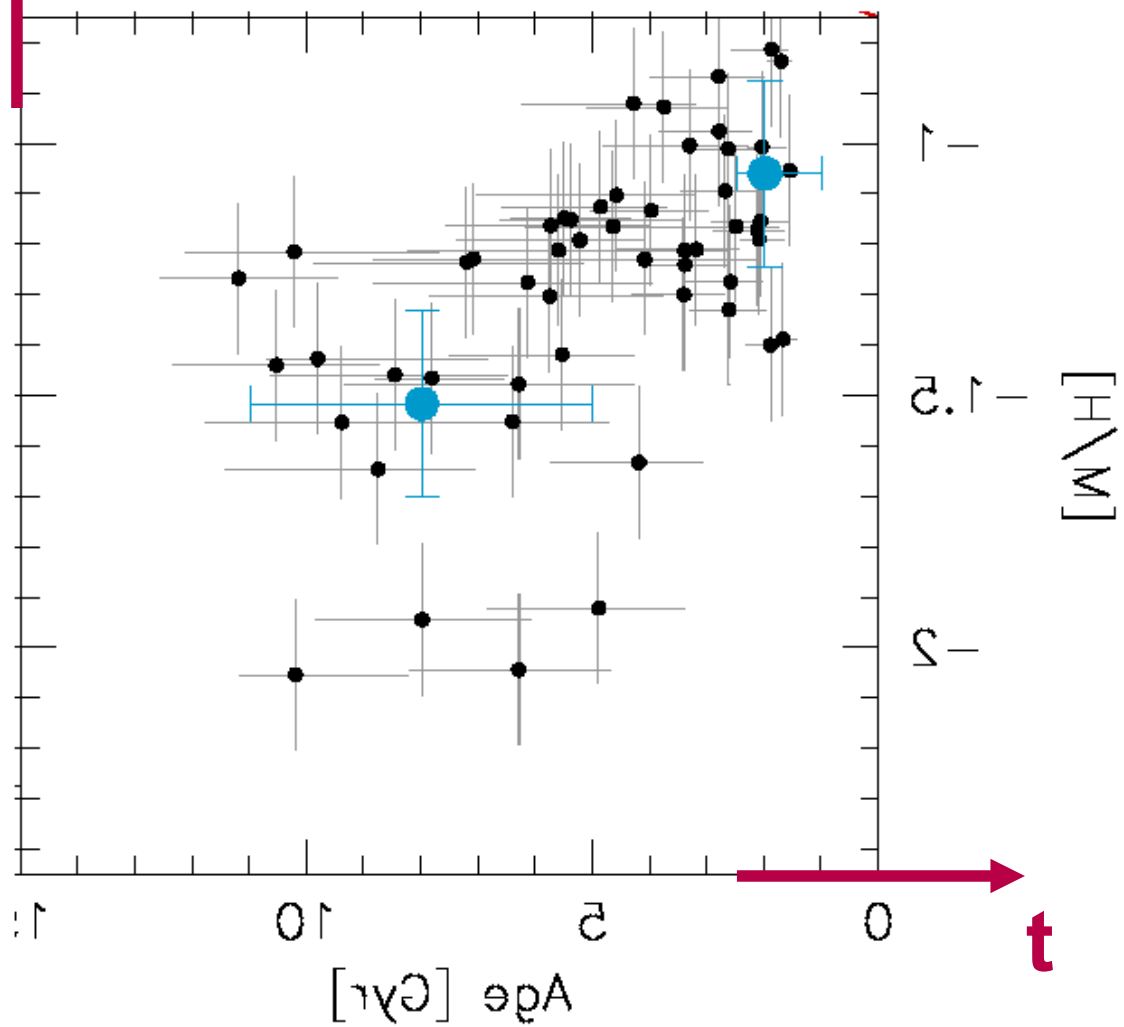


$$\frac{dN}{dZ} = \frac{M_{\text{tot}}}{m} \frac{1}{p} e^{-Z/p}$$

Leo I, Gullieuszik et al. 2009



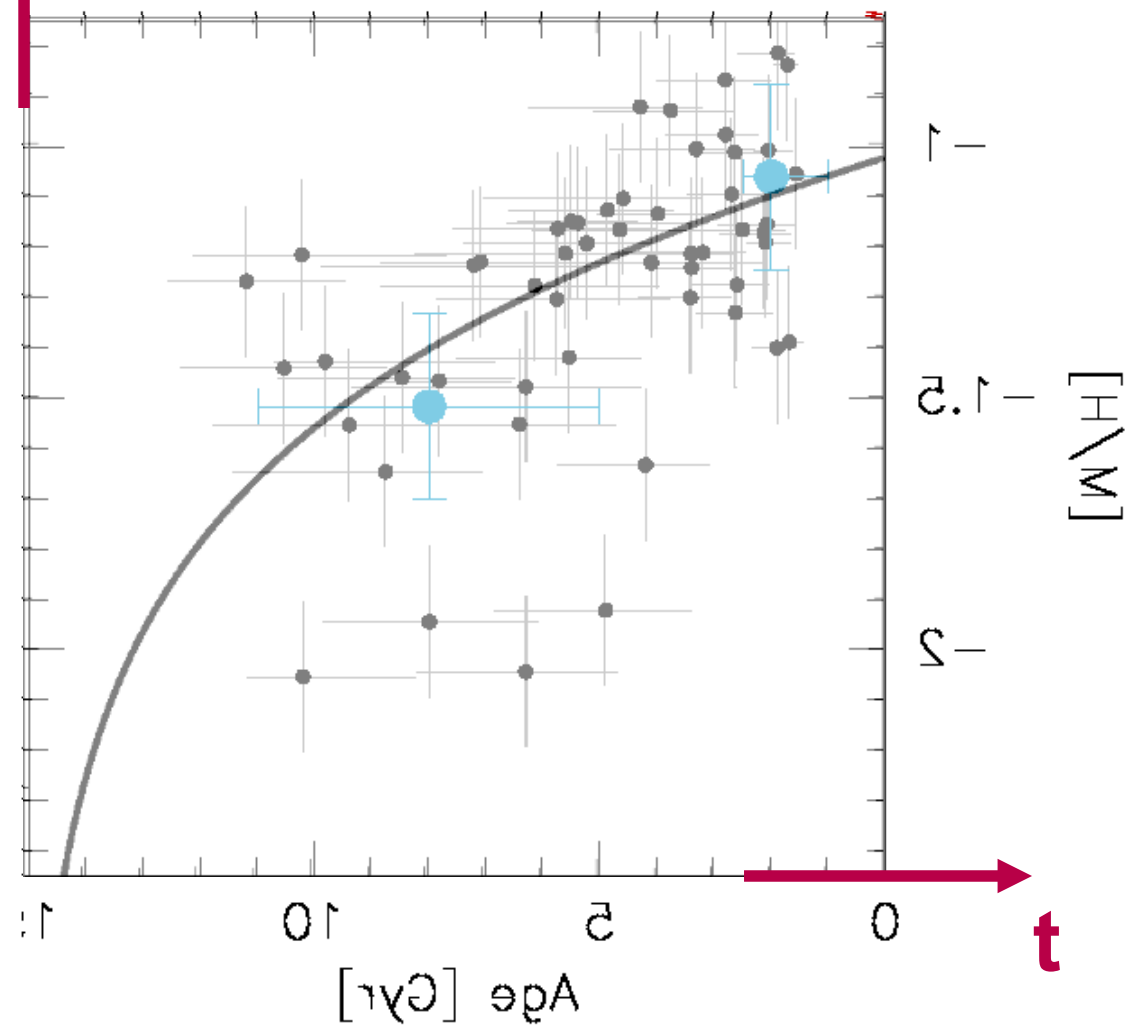
$\log(Z/Z_0)$



$\log(Z/Z_0)$

$$\frac{d\mu}{dt} = 0.2$$

$$p = Z_{\text{sun}}/2$$





Good luck from the LS site manager!





AUX



From Manu to here

How to get metallicities of resolved stellar populations, from the basics to methods for distant objects.
Or from detailed abundances of small samples to coarse abundances of large samples.



Our nearby universe

What is it?

Our lectures in this context



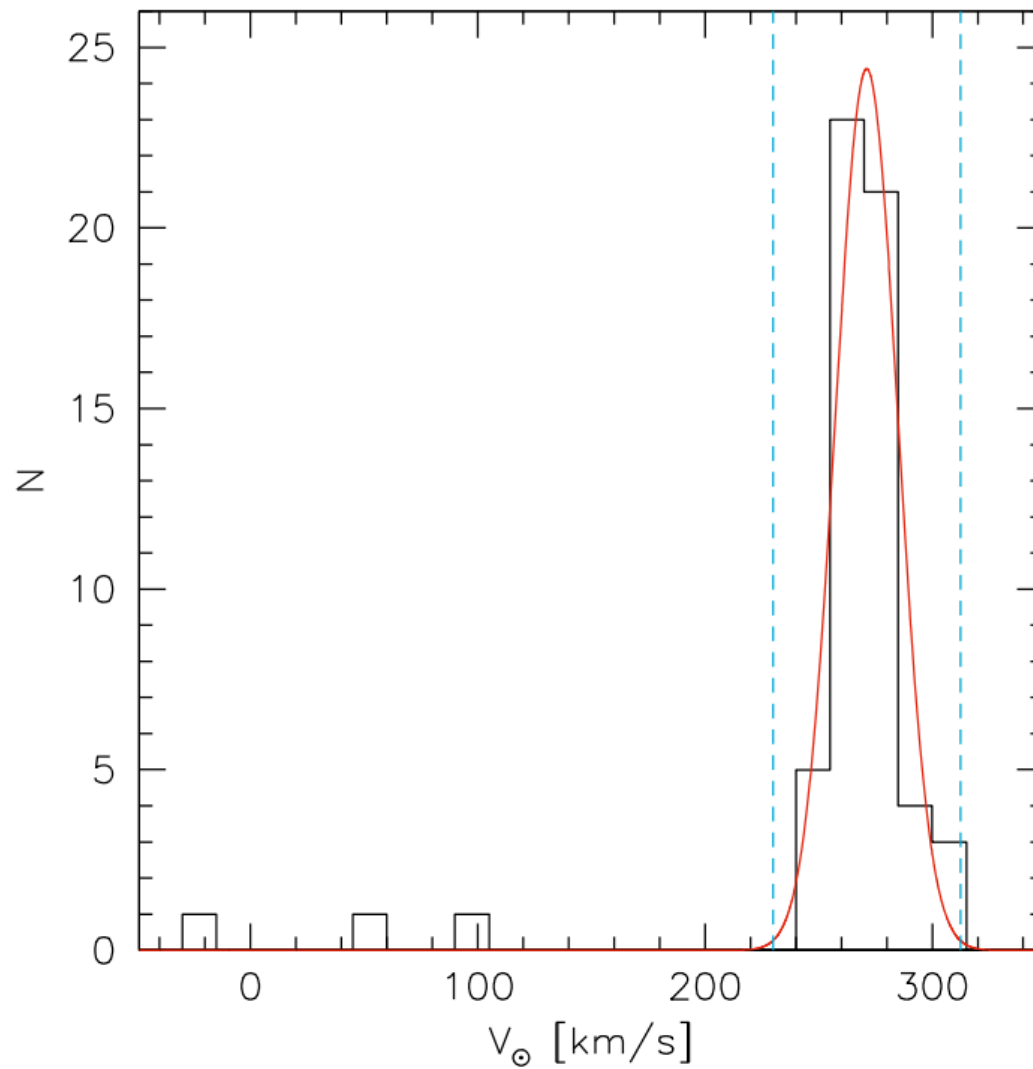
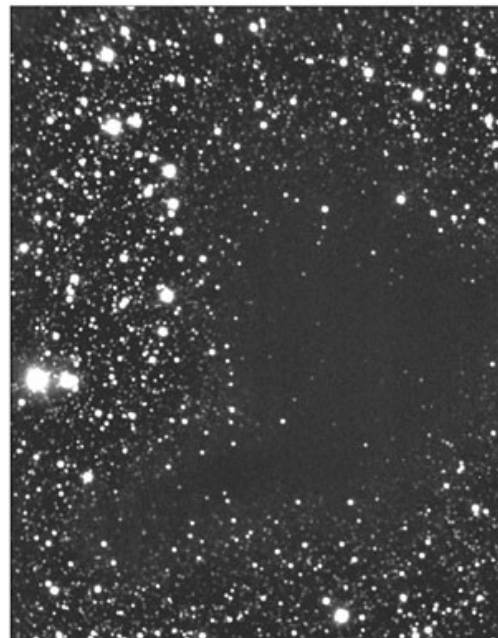
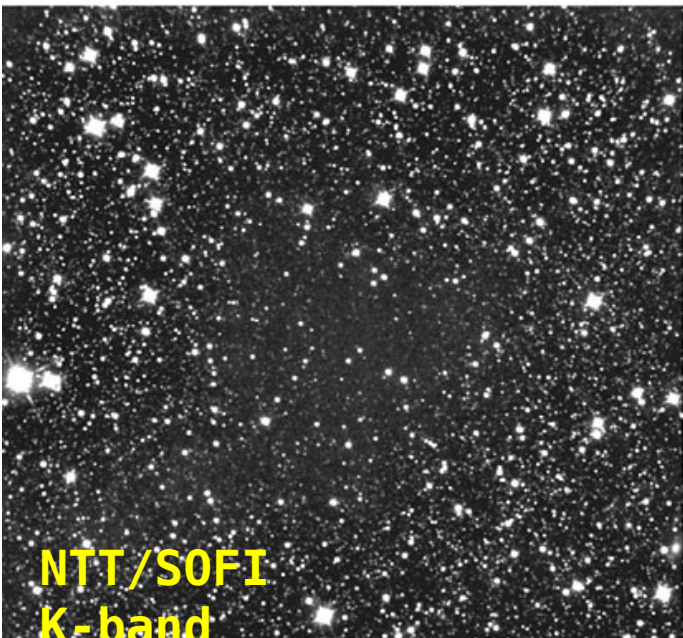
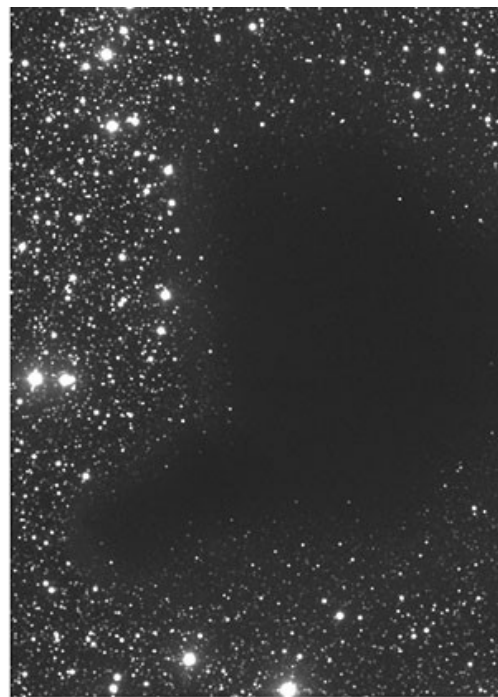
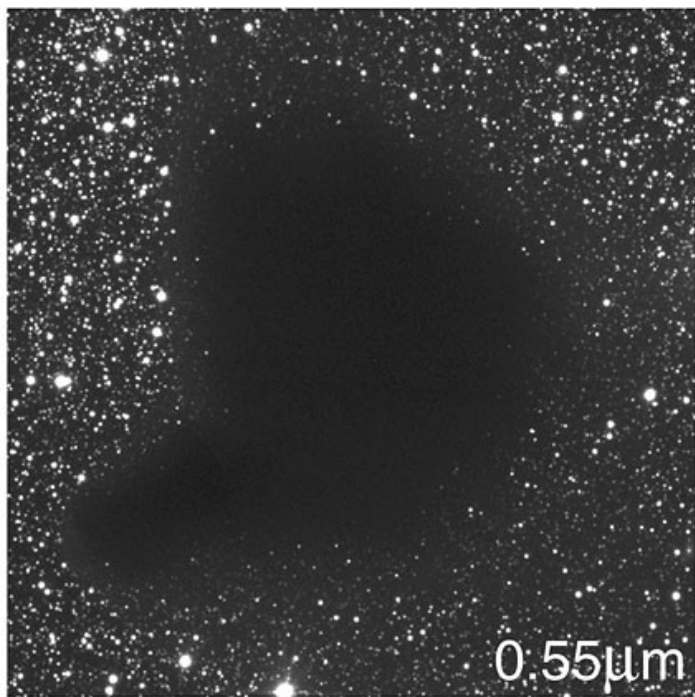
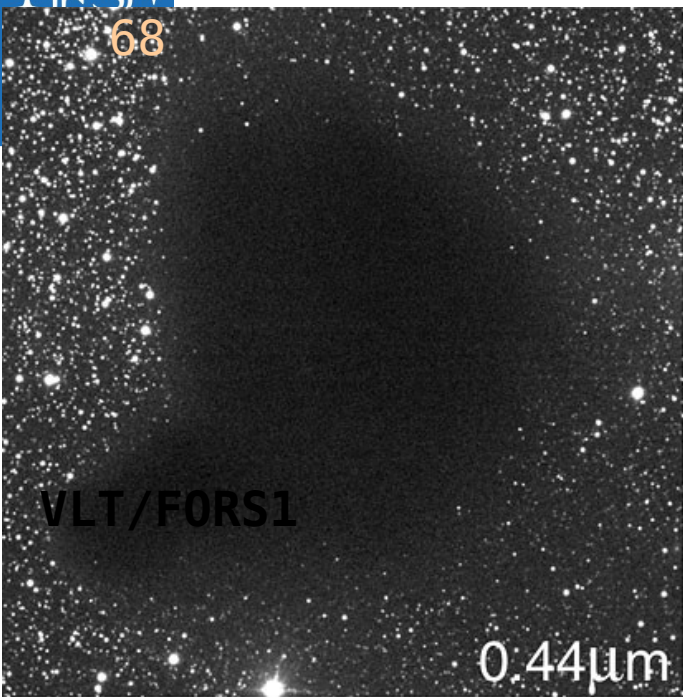
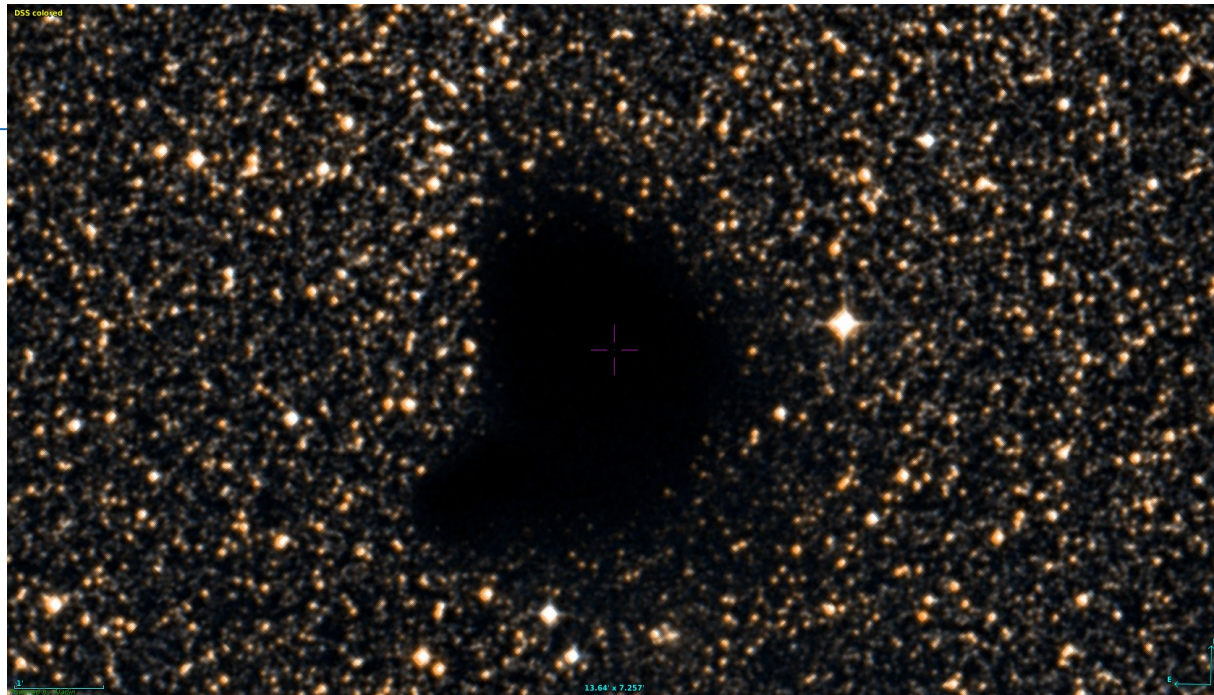


Fig. 4. Heliocentric radial velocities of stars in the Leo I field. The distribution is fitted with a Gaussian centred at 271 km s^{-1} and with dispersion 13.7 km s^{-1} . The vertical dashed lines represent the 3σ limits used to select members of Leo I.

Extension to NIR bands:

=> it does not matter how you compute $\langle W' \rangle$!





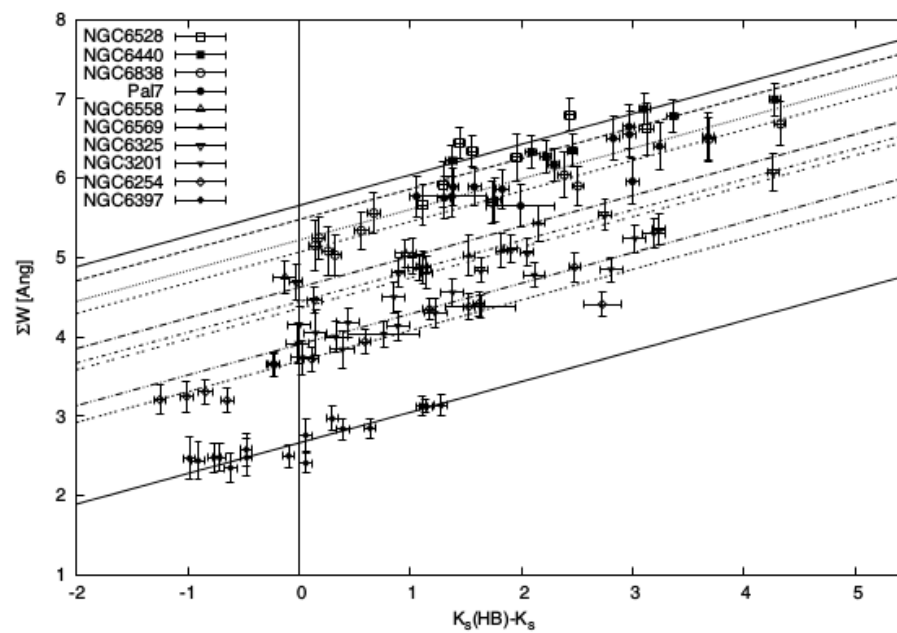
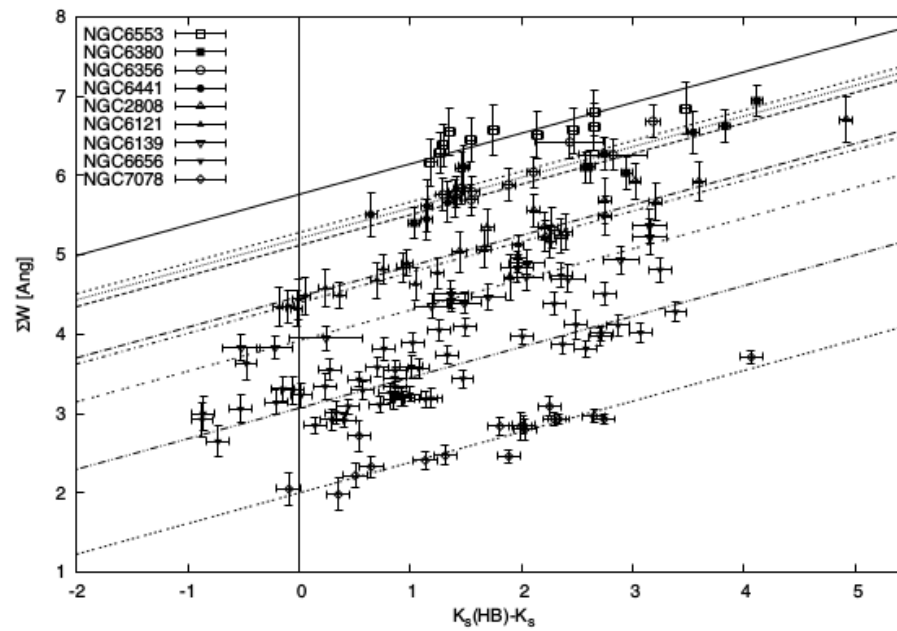


Fig. 3. Summed Ca II line strength $\sum W_{S12}$ plotted against magnitude difference from the red clump $K_s(\text{HB}) - K_s$ for the selected clusters.

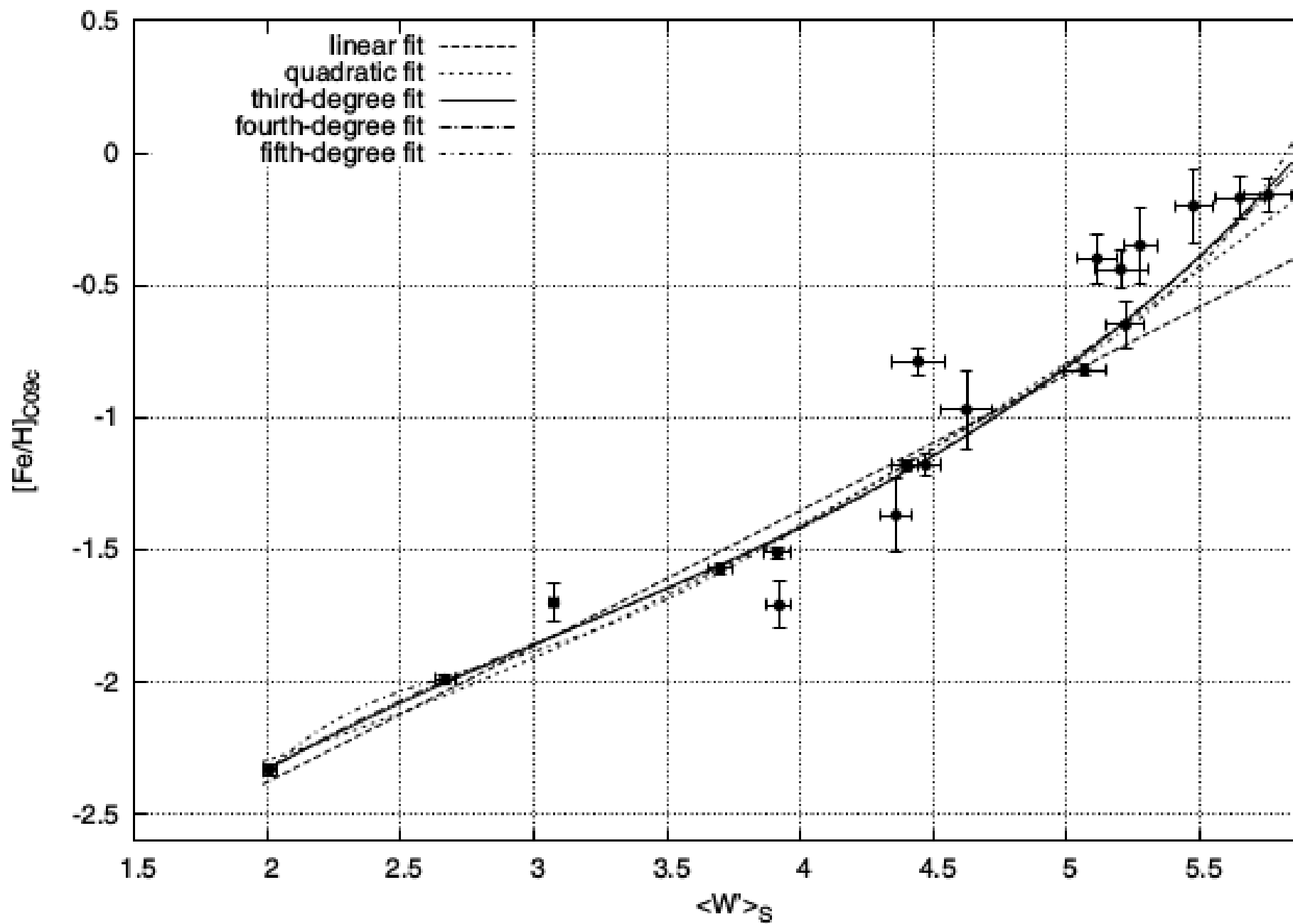


Fig. 5 Calibration relations between $[Fe/H]_{C08c}$ on the scale of Corcoran et al. (2008) and $\langle W \rangle_S$.

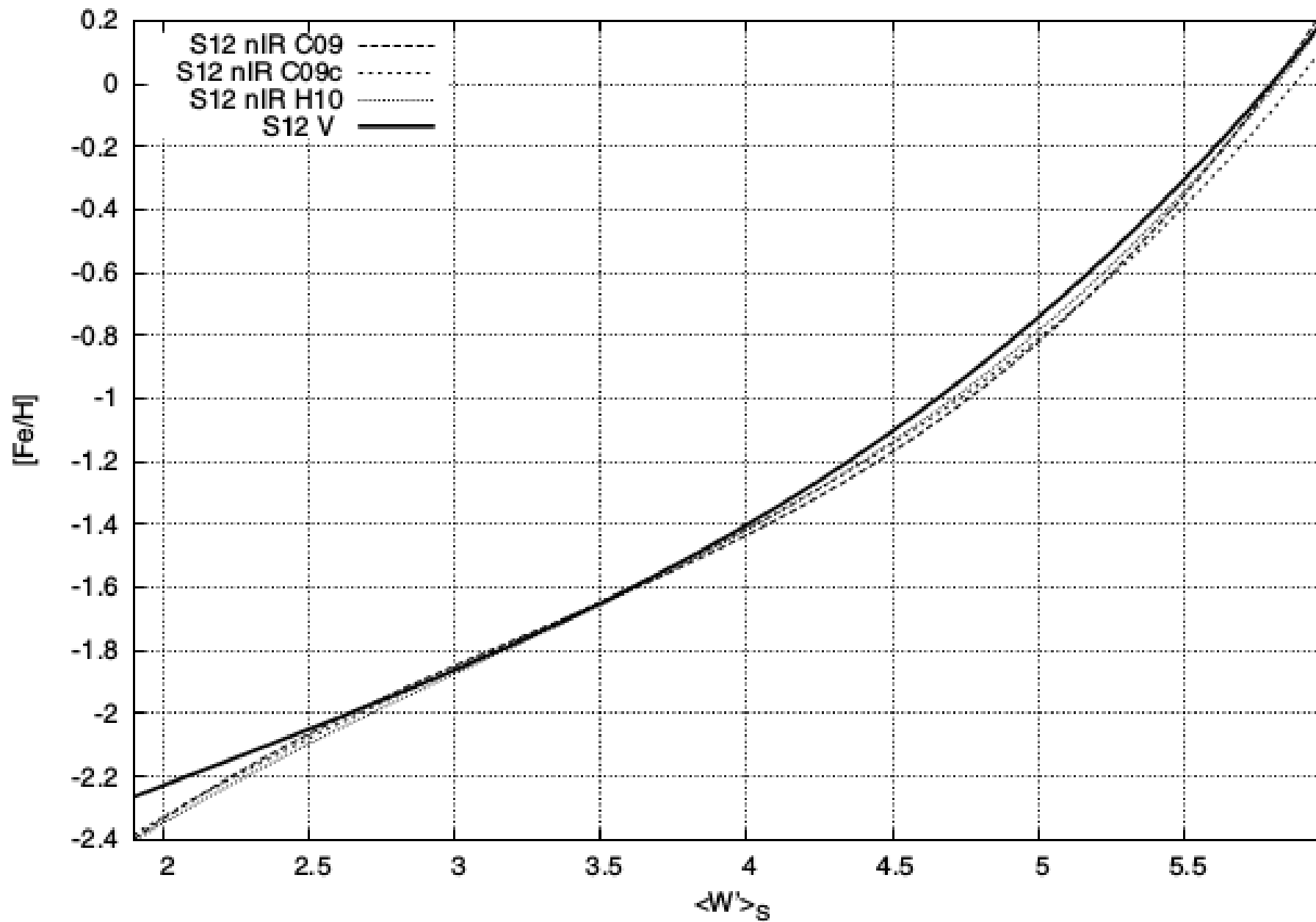
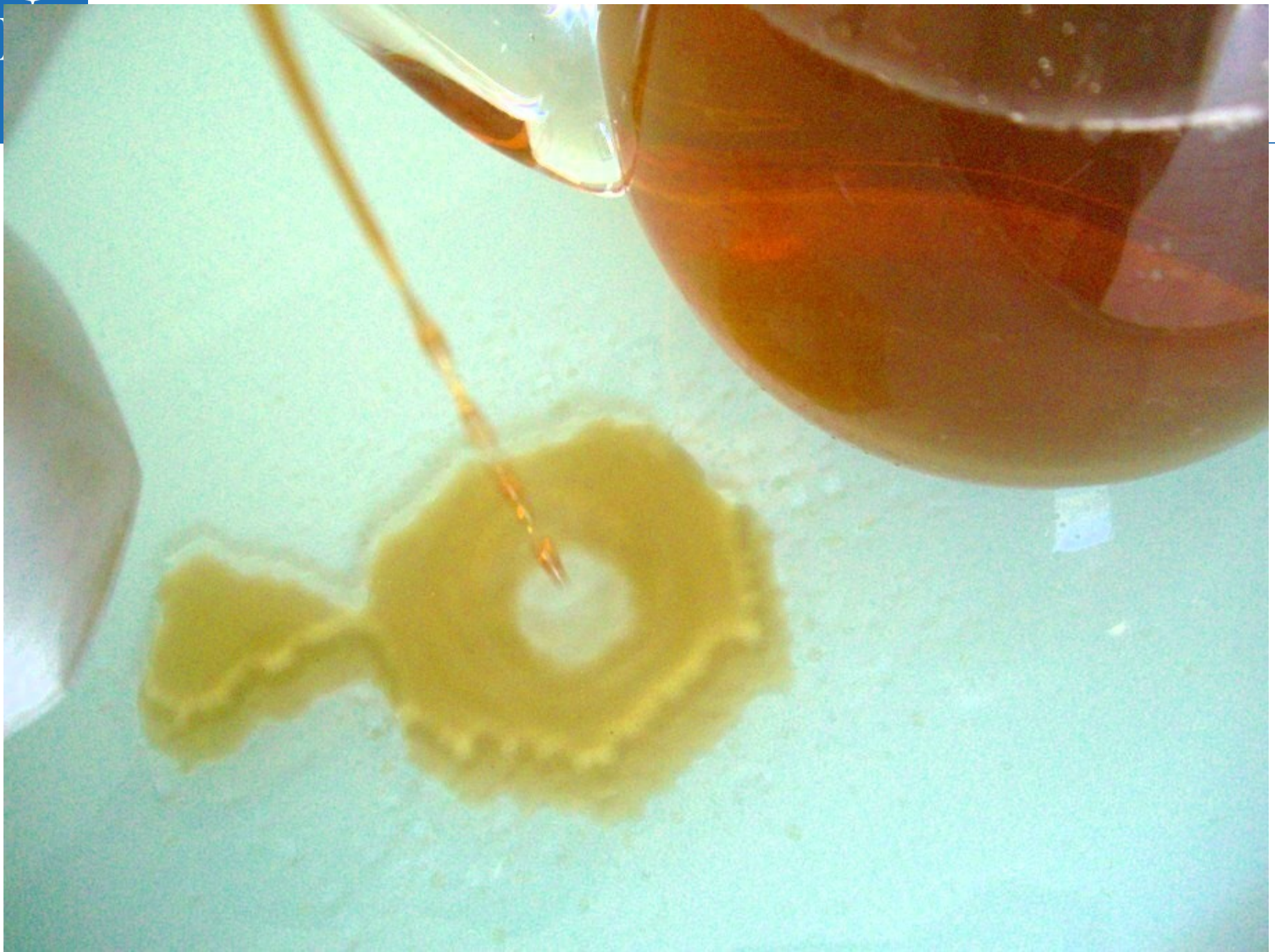


Fig. 7. Comparison of the cubic calibration relations [Fe/H] vs. $\langle W \rangle_S$.





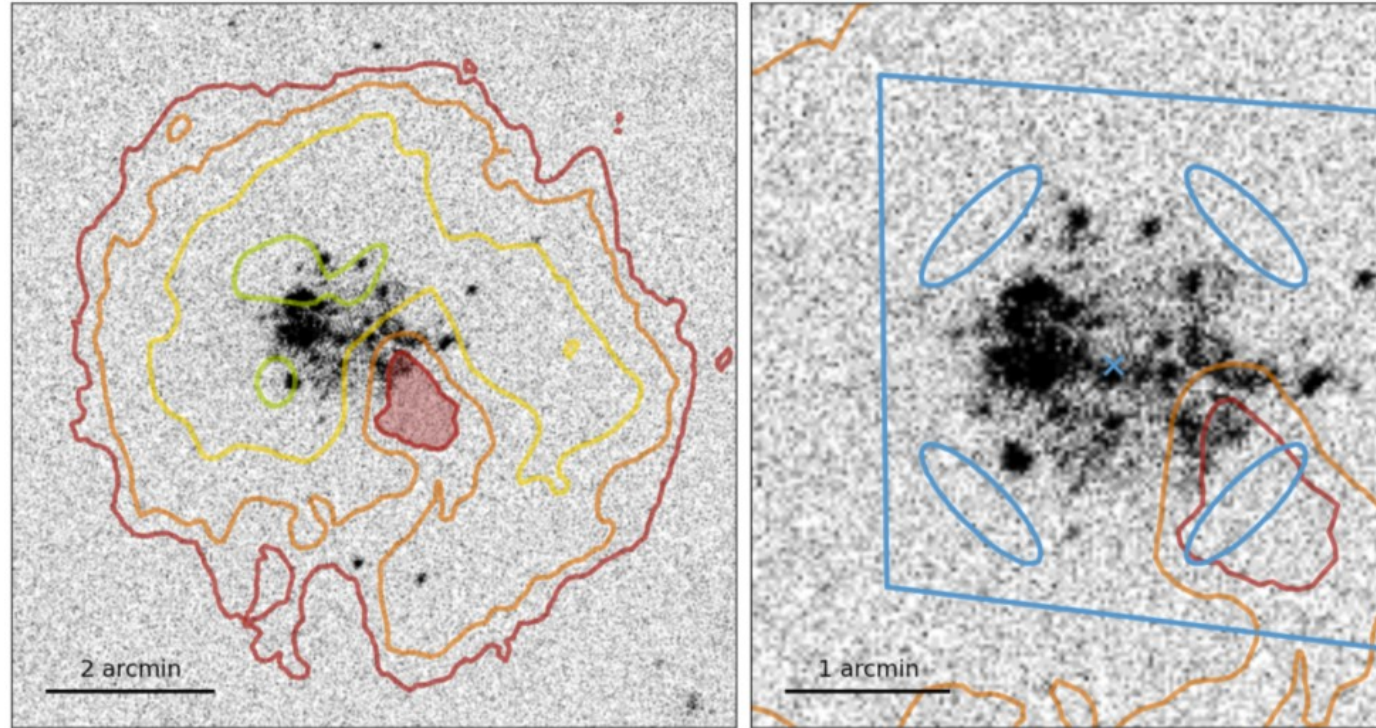
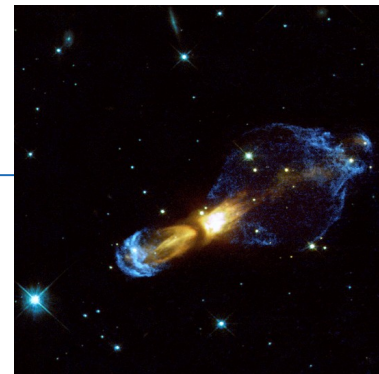


Fig. 5. GALEX far-ultraviolet image of SagDIG upon which HI contours are overplotted. The 3 highest density HI clumps are highlighted by the inner, open (green) contours, while the HI hole is highlighted by a shaded region. The *right panel* displays a closer view on the body of SagDIG highlighting (i) the quadrangle HST/ACS field of view; (ii) the SagDIG derived center (see text) marked by a cross and (iii) the 4 equidistant elliptical regions; used to extract and compare the stellar populations in the HI hole and the surrounding compact regions.

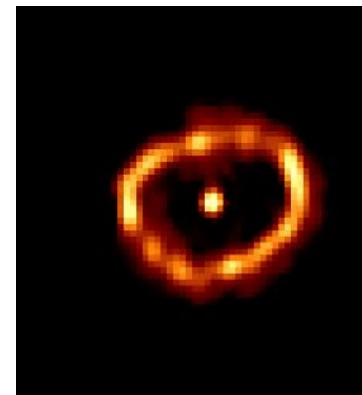




proto-planetary nebula
“rotten egg nebula”
HST/WFPC2



Nova Cygni 1992
Credit: NASA, ESA,
HST, F. Paresce,
R. Jedrzejewski
(STScI)



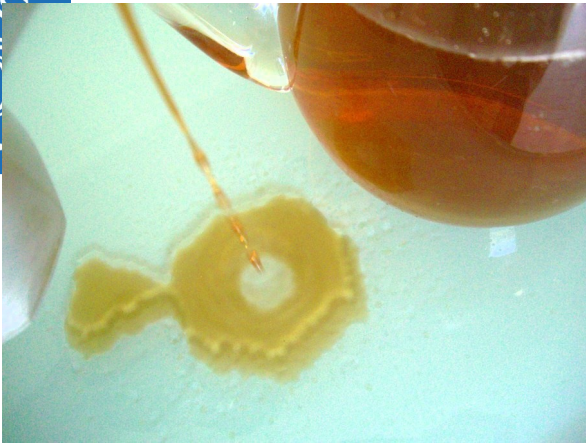
Wolf-Rayet
stars
e.g., Eta
Carinae



SN Type II
Type Ia

SN





M82: winds from a starburst galaxy





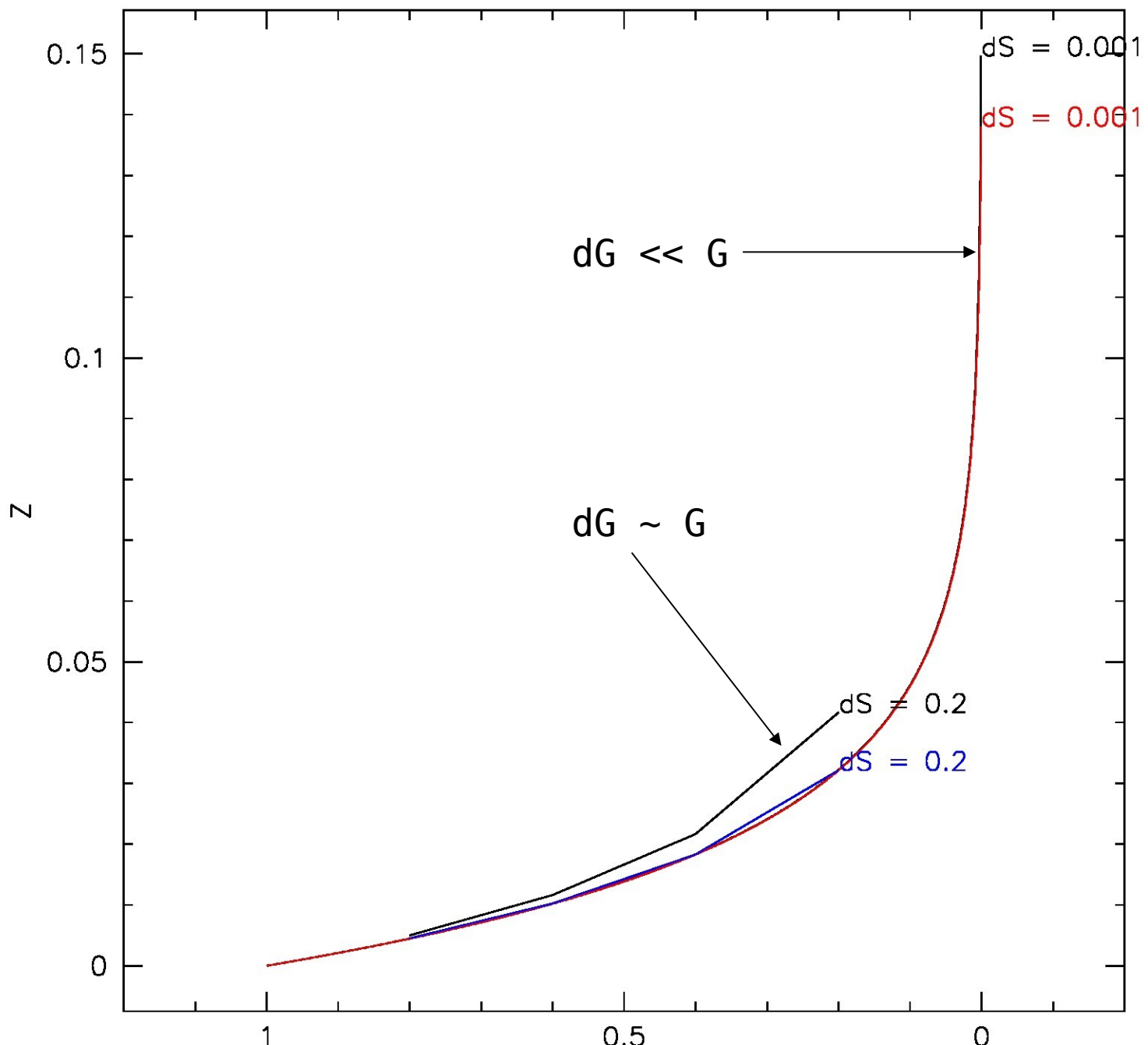
Better if gas-rich dwarf galaxy, like 

fixed

alpha-elements

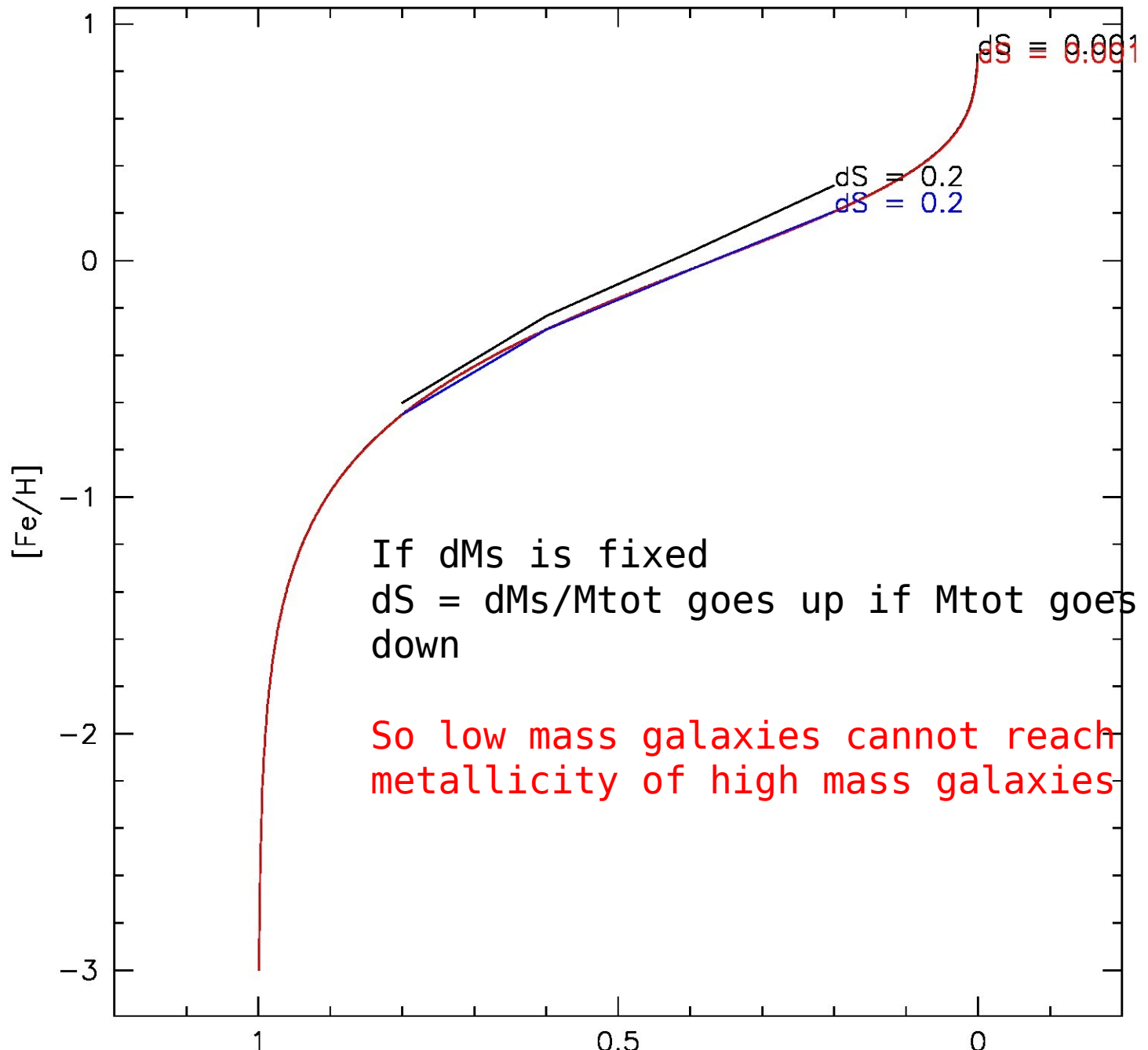


$p = 0.02$





$p = 0.02$





Fornax dSph; Pont et al. (2004)

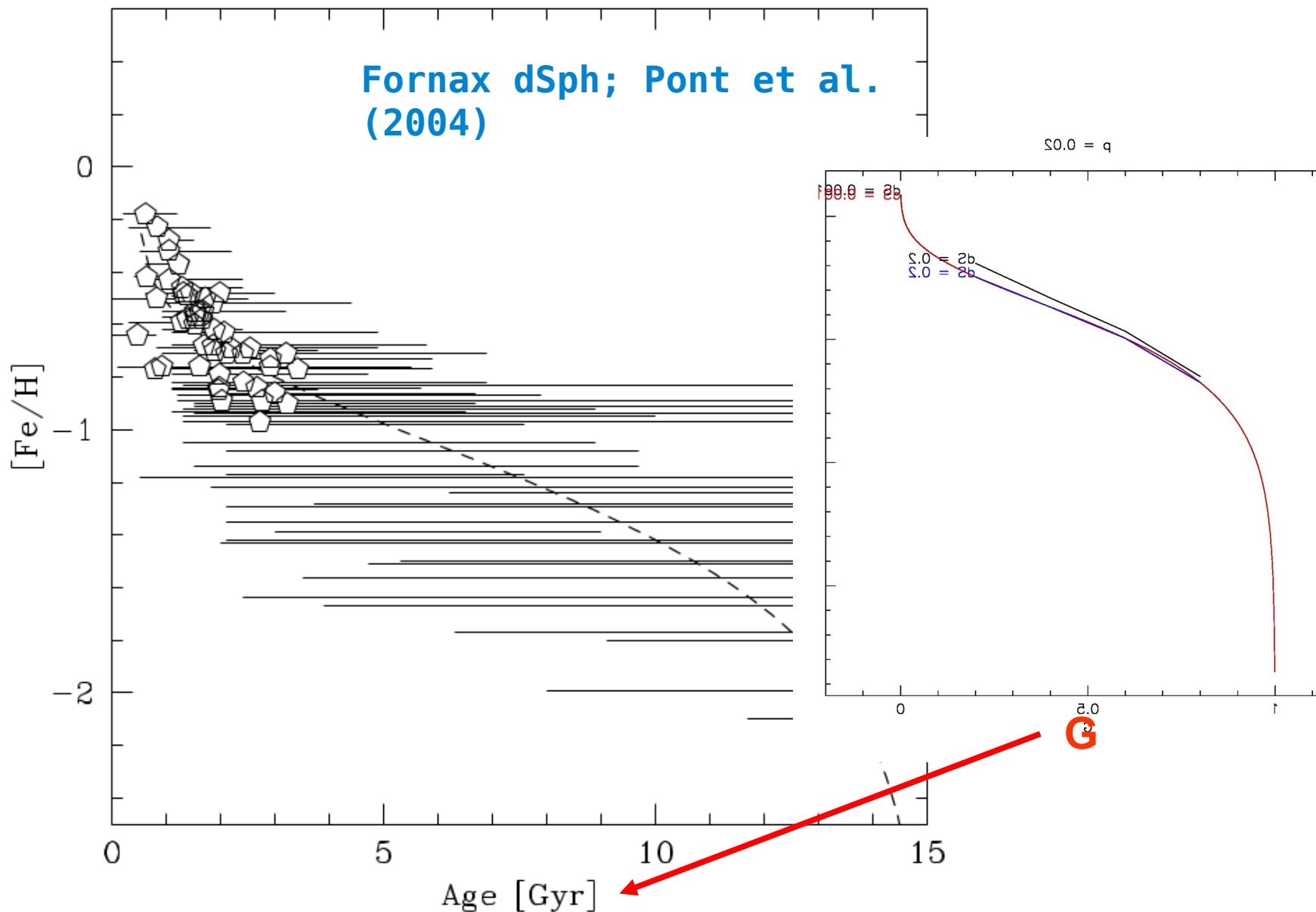


FIG. 11.—AMR of our sample. Ages derived by comparison with stellar evolution models of Girardi et al. (2000). The horizontal bars are the 95% age confidence intervals for each star. The most likely age is indicated by a

Assume $G(t)$
Age

